Cell Genomics

Article

Consequences of a telomerase-related fitness defect and chromosome substitution technology in yeast *synIX* strains

Graphical abstract

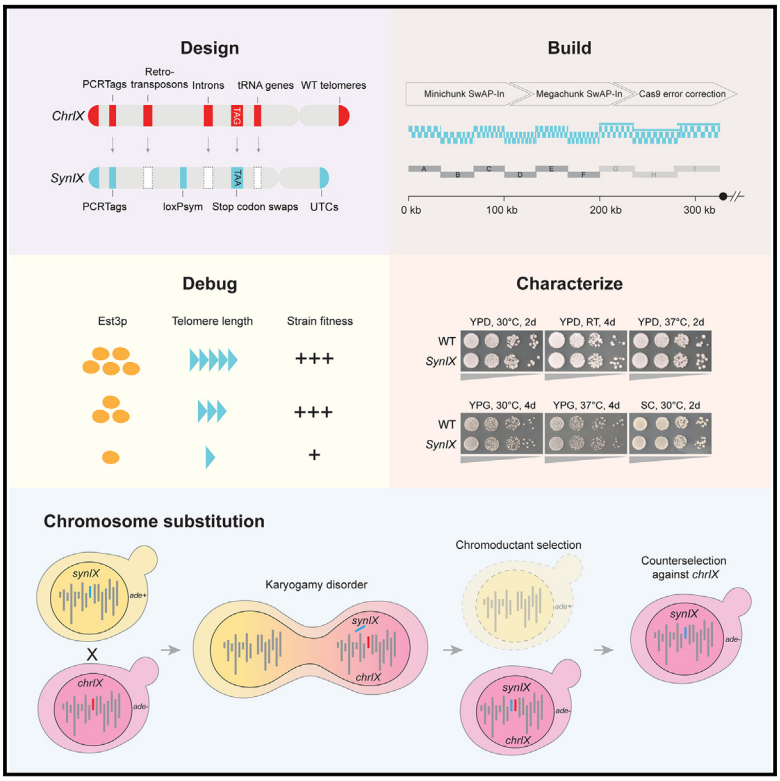

Highlights

- Following debugging, *synIX* shows high fitness under a variety of conditions
- An unusual bug resulting from a tRNA-associated deletion affects *EST3* expression
- Chromosome substitution method moves chromosomes to "fresh" genetic background

Authors

Laura H. McCulloch, Vijayan Sambasivam, Amanda L. Hughes, ..., Weimin Zhang, Jef D. Boeke, Srinivasan Chandrasegaran

Correspondence

weimin.zhang@nyulangone.org (W.Z.), jef.boeke@nyulangone.org (J.D.B.), chandra@jhmi.edu (S.C.)

In brief

McCulloch et al. describe complete synthesis of *synIX* and dissect a bug resulting from tRNA deletion upstream of telomerase-related *EST3* at the protein, RNA, and telomere length levels. A new genetic method, chromosome substitution, is used to swap *synIX* into alternative strains and can be broadly applied.

McCulloch et al., 2023, Cell Genomics *3*, 100419
November 8, 2023
https://doi.org/10.1016/j.xgen.2023.100419

CellPress

Cell Genomics

CellPress
OPEN ACCESS

Article

Consequences of a telomerase-related fitness defect and chromosome substitution technology in yeast *synIX* strains

Laura H. McCulloch,[1,22] Vijayan Sambasivam,[2,22] Amanda L. Hughes,[3] Narayana Annaluru,[2,17] Sivaprakash Ramalingam,[2,21] Viola Fanfani,[4,19] Evgenii Lobzaev,[4,5] Leslie A. Mitchell,[1,20] Jitong Cai,[6] The Build-A-Genome Class[6,7,8] Hua Jiang,[9] John LaCava,[9,10] Martin S. Taylor,[11]

(Author list continued on next page)

[1]Institute for Systems Genetics and Department of Biochemistry and Molecular Pharmacology, NYU Langone Health, New York, NY 10016, USA
[2]Department of Environmental Health and Engineering, Bloomberg School of Public Health, Johns Hopkins University, Baltimore, MD 21205, USA
[3]European Molecular Biology Laboratory (EMBL), Genome Biology Unit, 69117 Heidelberg, Germany
[4]School of Biological Sciences, The University of Edinburgh, Edinburgh EH9 3BF, UK
[5]School of Informatics, The University of Edinburgh, Edinburgh EH8 9AB, UK
[6]Department of Biomedical Engineering, Whiting School of Engineering, Johns Hopkins University, Baltimore, MD 21218, USA
[7]Department of Biology, Krieger School of Arts and Sciences, Johns Hopkins University, Baltimore, MD 21218, USA
[8]Department of Chemical and Biomolecular Engineering, Whiting School of Engineering, Johns Hopkins University, Baltimore, MD 21218, USA
[9]Laboratory of Cellular and Structural Biology, Rockefeller University, New York, NY 10065, USA
[10]European Research Institute for the Biology of Ageing, University Medical Center Groningen, Groningen, the Netherlands
[11]Department of Pathology, Massachusetts General Hospital, Harvard Medical School, Boston, MA 02114, USA
[12]Department of Medicine/Division of Infectious Diseases, Johns Hopkins University School of Medicine, Baltimore, MD 21205, USA
[13]High Throughput Biology Center, Johns Hopkins University School of Medicine, Baltimore, MD 21205, USA
[14]Stanford Genome Technology Center, Stanford University, Palo Alto, CA 94304, USA
[15]Department of Genetics, School of Medicine, Stanford University, Stanford, CA 94305, USA
[16]Department of Biomedical Engineering, NYU Tandon School of Engineering, Brooklyn, NY 11201, USA

(Affiliations continued on next page)

SUMMARY

We describe the complete synthesis, assembly, debugging, and characterization of a synthetic 404,963 bp chromosome, *synIX* (synthetic chromosome *IX*). Combined chromosome construction methods were used to synthesize and integrate its left arm (*synIXL*) into a strain containing previously described *synIXR*. We identified and resolved a bug affecting expression of *EST3*, a crucial gene for telomerase function, producing a *synIX* strain with near wild-type fitness. To facilitate future synthetic chromosome consolidation and increase flexibility of chromosome transfer between distinct strains, we combined chromoduction, a method to transfer a whole chromosome between two strains, with conditional centromere destabilization to substitute a chromosome of interest for its native counterpart. Both steps of this chromosome substitution method were efficient. We observed that wild-type *II* tended to co-transfer with *synIX* and was co-destabilized with wild-type *IX*, suggesting a potential gene dosage compensation relationship between these chromosomes.

INTRODUCTION

The Synthetic Yeast Genome Project (Sc2.0) marks a key milestone in the development of "designer" eukaryotic genomes. This global effort seeks to produce a modified version of the ~12 Mb *Saccharomyces cerevisiae* genome from the bottom up that retains native strain fitness while eliminating repetitive elements to improve genome stability and adding custom features to endow new genome functionalities. These changes include deletion of tRNA genes and introduction of loxPsym sites (symmetric, nondirectional *loxP* sites that can recombine with each other in two distinct orientations) downstream of nonessential

William R. Bishai,[12] Giovanni Stracquadanio,[4] Lars M. Steinmetz,[3,14,15] Joel S. Bader,[6,13] Weimin Zhang,[1,*] Jef D. Boeke,[1,13,16,23,*] and Srinivasan Chandrasegaran[2,18,*]

[17]Present address: L'Oréal Research and Innovation, Clark, NJ 07066, USA
[18]Present address: Pondicherry Biotech Private Limited, Pondicherry Engineering College Campus, East Coast Road, Pillaichavady, Puducherry 605014, India
[19]Present address: Department of Biostatistics, Harvard T.H. Chan School of Public Health, Boston, MA 02115, USA
[20]Present address: Neochromosome, Inc., Long Island City, NY 11101, USA
[21]Present address: Center for Scientific and Industrial Research, Institute of Genomics & Integrative Biology, Sukhdev Vihar, Mathura Road, New Delhi 110025, India
[22]These authors contributed equally
[23]Lead contact
*Correspondence: weimin.zhang@nyulangone.org (W.Z.), jef.boeke@nyulangone.org (J.D.B.), chandra@jhmi.edu (S.C.)
https://doi.org/10.1016/j.xgen.2023.100419

genes, enabling genome rearrangement via SCRaMbLE (synthetic chromosome rearrangement and modification by *loxP*-mediated evolution) and subsequent study of how different DNA sequence changes affect organismal fitness and function.[1–4] More broadly, by establishing a set of common design principles for all yeast chromosomes, Sc2.0 aims to provide a blueprint for future eukaryotic genome engineering endeavors. Each chromosome was redesigned and built from synthetic DNA blocks. Here, we report the assembly and characterization of synthetic chromosome *IX* (*synIX*), coinciding with completion of the assembly phase of Sc2.0 as a whole.[5–18]

Our group initially assembled a circular version of the right arm of the chromosome, *synIXR*, as a proof of principle for feasibility of the Sc2.0 project[6] and subsequently incorporated that chromosome arm into an otherwise wild-type and linear version of chromosome *IX*.[2] Here, we describe construction and characterization of *synIXL* and, consequently, the final version of *synIX*. As with many other completed Sc2.0 chromosomes and in accordance with Sc2.0 project objectives, *synIX*-containing strains, following a "debugging" process to resolve deficiencies in fitness across multiple growth conditions, behave similarly to the parental yeast strain with respect to fitness and transcriptional profiling.

Fitness defects have emerged during completion of many of the Sc2.0 chromosome strains. We attribute these growth issues, or "bugs," to a still-incomplete understanding of the *S. cerevisiae* genome during the initial design phase. Identifying and resolving such bugs may improve future genome engineering efforts and help anticipate and avoid potential complications. Bugs in previous Sc2.0 strains have commonly arisen from design choices (sequence additions, deletions, or modifications) that unexpectedly affected protein or RNA levels. For example, PCRTag recoding (intended to alter DNA sequence without changing amino acid sequence, producing watermarks to distinguish synthetic and wild-type sequences) lowered protein expression or interfered with transcription factor binding sites in other synthetic chromosomes.[7,9,11,12] Addition of loxPsym sites and removal of introns have affected RNA expression of genes in Sc2.0 strains, altering strain fitness.[7,11] For *synIX*, we identify and characterize a fitness defect related to a sequence adjacent to *EST3*, encoding a crucial yeast telomerase holoenzyme component involved in yeast telomere replication.[19–21] This bug resulted from a specific intentional design step, removal of a tRNA gene and associated repetitive DNAs. Deletion of a tRNA gene, Ty1 retroelement, and the DNA between them led to reduced average telomere length and impaired strain growth at higher temperature (37°C), a likely consequence of significant Est3p reduction. Reintroduction of part or all of this sequence dramatically improved fitness. Our experiments dissecting this bug show that Est3p expression levels were markedly reduced following deletion of an upstream tRNA gene and associated sequences per the chromosome's design; reinsertion of the tRNA gene and associated sequences in various configurations led to partial or total restoration of both Est3p levels and telomere length. We suggest that a minimum threshold Est3p level suffices to restore telomere length, supporting near-normal fitness at 37°C.

The ultimate goal of Sc2.0 is to create a high-fitness yeast strain with a fully synthetic genome. A previously described chromosome consolidation method relying on chromosome endoreduplication followed by sporulation becomes laborious and time consuming as synthetic chromosome number increases.[2,22] Here, we present a strategy combining chromoduction of *synIX* and subsequent loss of native chromosome *IX* (*chrIX*) to accelerate consolidation. This approach takes advantage of a karyogamy defect arising when either parent in a cross carries a *kar1-1* mutation.[23] Such crosses yield heterokaryons consisting of nuclear material from one yeast strain with mixed cytoplasm of the parent strains. In rare cases, whole chromosomes transfer between strains in a *kar1-1* x *KAR1* cross.[24] While chromoduction occurs more frequently with smaller chromosomes,[24] prior work has employed a selection strategy to identify chromoductants in which a particular chromosome has been transferred.[25,26] Conversely, whole-chromosome destabilization can be achieved by activating a *GAL* promoter immediately upstream of yeast centromeres.[7,27] Here, we demonstrated the feasibility of synthetic chromosome transfer using *synIX*, producing a final haploid yeast strain in which *synIX* has replaced wild-type *chrIX*. This represents a promising proof of principle for targeted transfer of chromosomes among yeast strains; indeed, this method is used in final consolidation of Sc2.0 chromosomes into a single yeast strain.[22]

RESULTS

Design and assembly of *synIX*

SynIX adheres to Sc2.0 project principles.[2] The designed *synIX* sequence contains a variety of modifications, including deletion of ten tRNA genes (relocated to a separate tRNA

neochromosome) and 11,632 bp repetitive DNA; recoding of 54 stop codons from TAG to TAA, 436 bp restriction enzyme sites, and 7,943 bp PCRTags; and addition of 142 loxPsym sites downstream of nonessential genes allowing for the Cre-mediated SCRaMbLE system (Figure 1A).[1–4] These changes reduced the *chrIX* length from 439,885 to 404,963 bp in *synIX*.

Following synthesis of *synIXR*,[6] we began construction of *synIXL* using a strain containing a linear, partially synthetic chromosome *synIXR* with a native left arm (yLM461).[2] Assembly of *synIXL* proceeded in several stages (Figure 1B). Initially, we assembled 750 bp building blocks from synthetic 60–70 bp oligonucleotides through polymerase cycling assembly (PCA) in the context of the Build-A-Genome undergraduate class (Figure S1A).[5,6] We then combined these building blocks to form 2–4 kb minichunks. In later project stages, as DNA synthesis technology improved and costs dropped, we obtained the remaining minichunks directly from a vendor.

We divided *synIXL* into nine 30–60 kb megachunks, each comprising minichunks that overlapped adjacent ones. To assemble the first six megachunks (A–F), we transformed component minichunks into our entry strain one megachunk at a time, adding an auxotrophic marker to each distal minichunk (Figure 1C). Through yeast homologous recombination, each assembly step overwrote the native segment and adjacent auxotrophic marker with synthetic DNA and a new auxotrophic marker in accord with the switching auxotrophies progressively for integration (SwAP-In) method,[2,6] enabling selection of strains containing newly integrated DNA (Figure 1C; Table S1). After each integration round, the PCRTag watermarking system allowed identification of colonies with synthetic DNA and lacking wild-type DNA (Table S2).

The minichunk integration approach used in assembling megachunks A–F left some unwanted patches of wild-type *chrIX* sequence (Figure 1B, top). To improve efficiency and avoid such wild-type DNA patches, later *synIXL* sections used the "megachunk-BAC" integration strategy.[12] For these sections, we first assembled minichunks into 40–60 kb megachunks (megachunks G–I) as extrachromosomal bacterial artificial chromosomes (BACs) in yeast, with assembly success rates of 20%–45% (Figure 1D; Table S3), and subsequently transformed them into *E. coli* for plasmid extraction. Following megachunk-BAC sequence verification, these megachunks were released from their plasmid backbones using restriction enzyme digestion and delivered directly into the semisynthetic (A–F) *synIX* strain for SwAP-In. We verified successful integration of megachunks G–I via whole-genome sequencing; all three were fully integrated into the *synIX* strain and lacked novel mutations and wild-type sequences (Figure 1B, middle).

To convert wild-type DNA patches seen in megachunks A–F to synthetic, we used CRISPR-Cas9 editing to selectively target *synIX* at residual *chrIX* PCRTags within each patch (Figure S1B) and repaired them with appropriate synthetic donor DNAs.[9,10] Following replacement of ten minichunks over seven rounds of CRISPR-mediated editing, we obtained a version of *synIX* containing all synthetic segments as designed (Figure 1B, bottom; Table S4).

We continued CRISPR-mediated editing of this "draft" strain to correct point mutations, small deletions, and duplications in *synIX*, detailed in Table S5. Additionally, we discovered a discrepancy stemming from inaccuracies in the yeast reference genome sequence originally used in *synIX* design; the sequence for (nonessential) *FAA3* contained an extra 7 bp absent from the updated reference sequence, resulting in a frameshift (Figure 1E).[28,29] A previous genetic screen linked *faa3Δ* to decreased growth[30]; consequently, we restored proper *FAA3* function in our *synIX* strain by reestablishing the updated *FAA3* reading frame (Figure S2).

During this process, we unexpectedly identified whole-chromosome disomy of *synIX* (Figure 1F, top). To restore the normal karyotype, we integrated a *URA3-pGAL* cassette upstream of *CEN9* into one *synIX* copy[27] and induced chromosome destabilization (Figure S3). Whole-genome sequencing confirmed that the resulting *synIX* strain contained approximately equal read depth for each chromosome, as expected for a monosomic haploid yeast strain (Figure 1F, bottom). There were no overt phenotypic differences between the disomic and monosomic strains, suggesting that the disomy was an inadvertent consequence of CRISPR-mediated editing rather than selection for a second copy of *synIX* due to haploinsufficiency. This monosomic strain was used for further debugging.

Debugging of *synIX*

After correcting the above *synIX* sequence issues, we found that this strain, coined yeast_chr09_9_1 (also referred to as yLHM1192), grew less well than the parental strain at 37°C on both YPD and YPG media (Figure 2A). A similar phenotype was observed in additional yLHM1192-equivalent strain isolates (Figure S4). Following a pooled sequencing bug mapping method,[9] we backcrossed the *synIX* strain to a wild-type strain to generate a heterozygous diploid yeast strain for sporulation and subsequently dissected tetrads. Spores contained a randomized mixture of recombinant *synIX* and *chrIX* DNA resulting from meiotic recombination (Figure S5A). By conducting whole-genome sequencing of healthy and sick spores, we identified a region spanning ~15–20 kb upstream of *CEN9* to 5 kb downstream of *CEN9* associated with the fitness defect (Figures 2B and S5B). Consistent with this mapping, the *synIX* strain initially exhibited a marked decline in fitness following integration of megachunk I, containing the corresponding synthetic sequence (Figure S6). To determine the gene responsible, we cloned each gene in this region into a *CEN* plasmid for complementation testing (Figure S7). Strains containing a plasmid with *EST3* showed a pronounced fitness improvement on both YPD and YPG media at 37°C compared with the buggy *synIX* strain (Figures 2B and S7).

To investigate which modifications of the synthetic *EST3* region might reduce fitness, we replaced sections of the synthetic region with corresponding wild-type sequences in our *synIX* strain and monitored growth. Replacing *EST3* coding sequences did not restore fitness (Figure 2C, yLHM1429); however, additionally restoring a deleted segment upstream of *EST3* containing a $tRNA^{Asp}$ gene and a nearby Ty1 long terminal repeat (LTR) element dramatically improved *synIX* strain fitness (Figure 2C, yLHM1430 and yLHM1431). To better assess the contributions of these *EST3*-adjacent elements to fitness, we introduced smaller modifications to *EST3*'s upstream region in the *synIX* strain, including different combinations of the $tRNA^{Asp}$

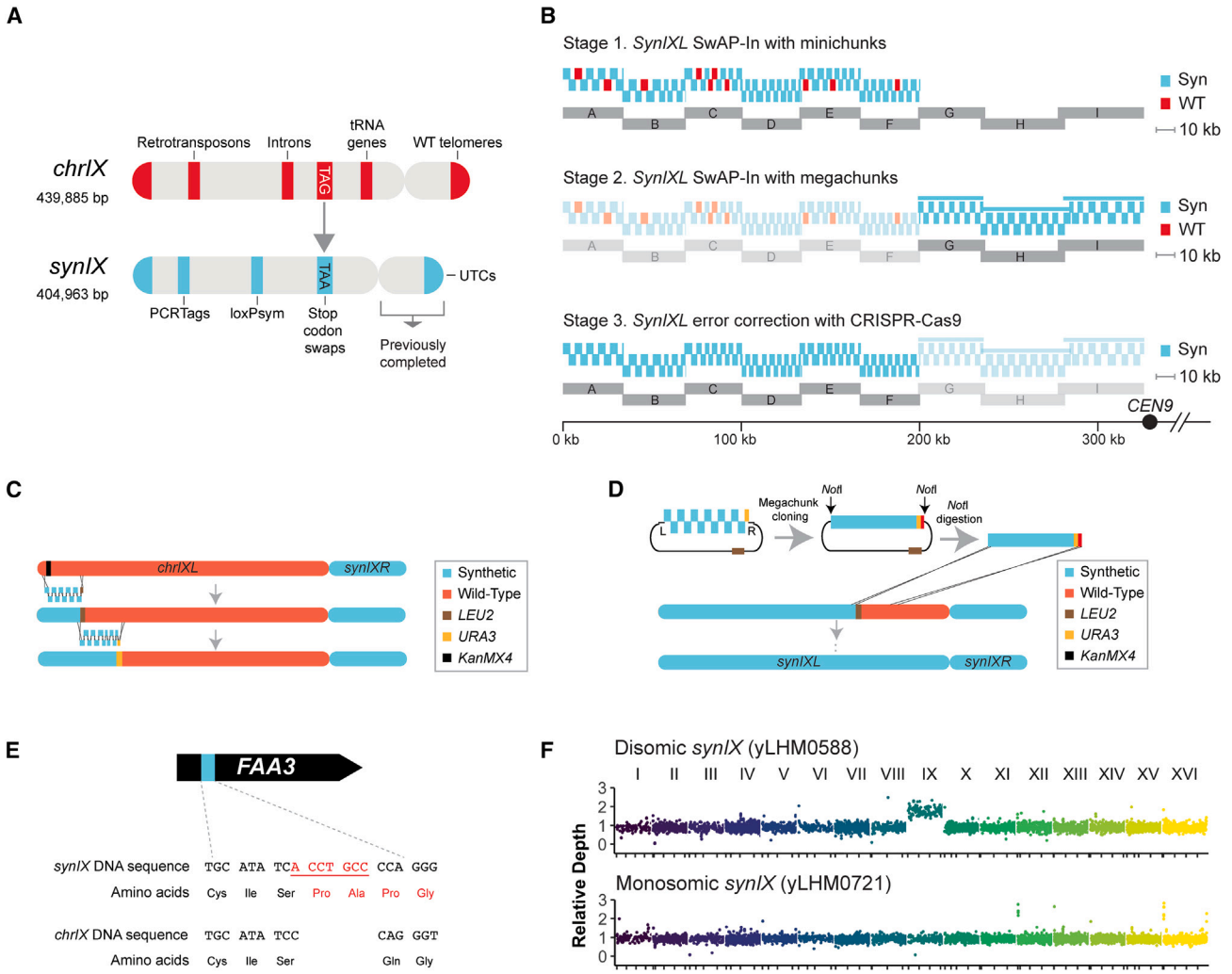

Figure 1. Design and assembly of *synIX*

(A) Diagram of the differences between wild-type (WT) *chrIX* and *synIX*. Designer features specific to *synIX* include addition of PCRTags and loxPsym sites, recoding of TAG stop codons to TAA, replacement of WT telomeres with universal telomere caps (UTCs), and removal of tRNA genes (relocated to a tRNA neochromosome), introns, retrotransposons, and subtelomeric repeats.

(B) Schematic of the *synIXL* construction process, reflecting synthetic and (unwanted) WT composition of *chrIX* in the *synIX* strain after each stage of assembly. Stage 1: SwAP-In with minichunks (A–F). Stage 2: SwAP-In with preassembled megachunks (G–I, opaque with blue lines). Stage 3: error correction with CRISPR-Cas9 (primarily in highlighted megachunks A–F). Blue: syn minichunks, red: WT minichunks, gray: megachunks. Red patches in stages 1 and 2 reflect segments of DNA that were not replaced by their expected synthetic minichunk counterparts during SwAP-In with minichunks in stage 1 (A–F); appropriate synthetic sequences were integrated at these sites during stage 3. kb, kilobase pairs.

(C) Minichunk integration strategy for assembling megachunks A–F of *synIX* in yeast (used for stage 1 in B). KanMX marker (black) was integrated into left end of WT *chrIX* (red). Individual minichunks (blue, synthetic) comprising one megachunk were then co-transformed into in-progress *synIX* strain and used to overwrite WT *chrIX* sequence (red) via homologous recombination. Alternating auxotrophic markers (*LEU2*, brown, and *URA3*, orange) were used and overwritten at each step.

(D) Megachunk plasmid assembly and integration approach for building and integrating megachunks G–I in *synIX* (used for stage 2 in B). Minichunks (blue) were assembled in yeast, and an auxotrophic marker (here, *URA3*, orange) was added to the end of each assembly, followed by a segment of *chrIX* homology. Megachunk assembly overwrote prior round auxotrophic marker (brown, *LEU2*) and WT DNA (red) by homologous recombination.

(E) Schematic depicting frameshift mutation in *FAA3* gene in *synIX* design. Synthetic sequence included 7 bp not present in S288C WT yeast reference genome. Added bases (red) cause a frameshift, with resulting *synIX* amino acid sequence (red) varying from the expected *chrIX* amino acid sequence (black, bottom).

(F) Coverage plots showing read depth along each yeast chromosome in disomic *synIX* strain yLHM0588 (top) and monosomic *synIX* strain yLHM0721 (bottom). The x axis: yeast chromosome (not to scale). The y axis: relative depth based on number of reads at each position divided by average read depth across sixteen yeast chromosomes.

See also Figures S1–S3 and Tables S2, S3–S5, and S8.

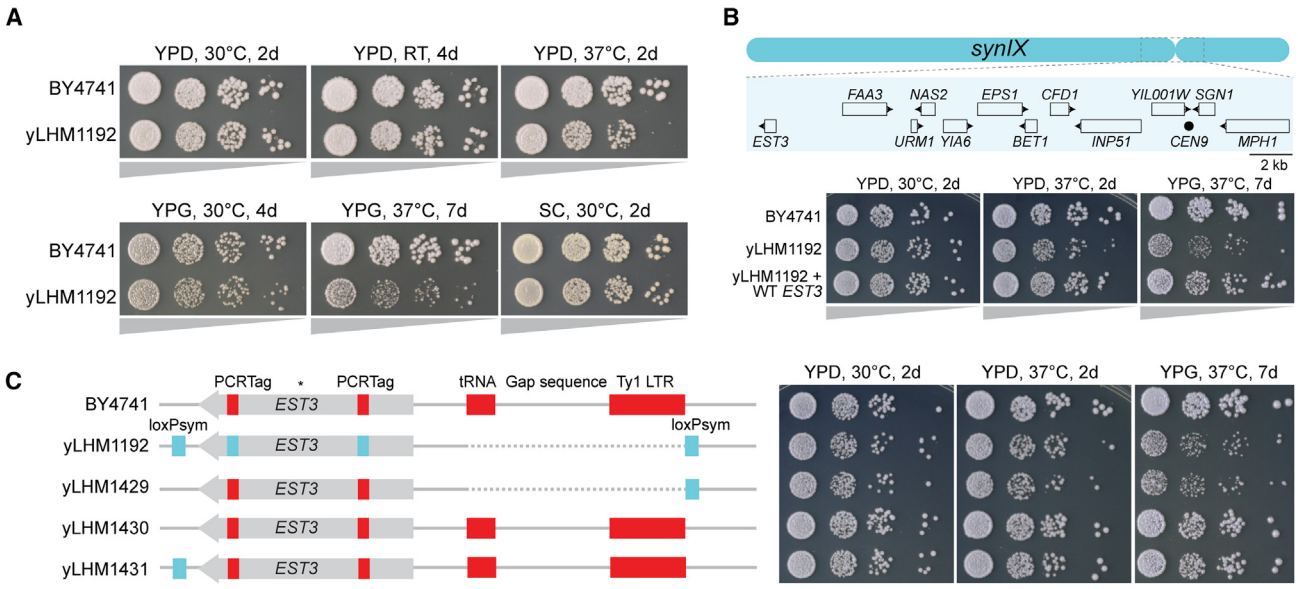

Figure 2. Identifying and mapping an *EST3*-related bug

(A) Spot assays comparing the growth of BY4741 (WT) to yLHM1192 (synthetic) across a variety of growth conditions. Each column represents a 10-fold dilution. RT, room temperature, ~22°C.

(B) (Top) Schematic of region near *CEN9* identified as containing gene responsible for *synIX* fitness defect. Unhealthy *synIX* strain (yLHM1192) was transformed with plasmids containing transcription units for each gene shown. (Bottom) Spot assays comparing growth of BY4741 and yLHM1192 to yLHM1192 transformed with plasmid containing *EST3* coding sequence plus 500 bp upstream sequence and 200 bp downstream sequence. Each column represents a 10-fold dilution.

(C) Spot assays comparing growth of strains with different combinations of synthetic and WT features in and upstream of *EST3*. Each column represents a 10-fold dilution. Schematics on the left illustrate WT (red) and synthetic (blue) features present in each strain. Asterisk (*) marks site of known *EST3* programmed +1 ribosomal frameshift.

See also Figures S4–S7.

gene, a nearby Ty1 LTR, and an intervening single-copy "gap" DNA sequence with no known function (Figure 3A; Table S6). All of these edits improved strain fitness (Figure 3A). Similar phenotypes were observed in additional strains generated for each modification and did not noticeably change following extended strain passaging (Figure S8).

As *EST3* is involved in telomere maintenance,[19–21] we hypothesized that *EST3*-associated changes in fitness might correlate with changes in average telomere length. We assessed telomere length of *synIX* and variant strains via southern blotting using a probe specific for telomeric repeats (Figure 3B). Following enzymatic digestion of yeast gDNA with *Xho*I, a smear of small telomeric fragments from chromosome ends containing Y′ elements is seen in each lane; these fragments were used to estimate average telomere length, with other telomeric fragments appearing at larger sizes. As expected, yLHM1192's telomeres were markedly shorter than those seen in the wild-type BY4741 strain. Interestingly, the telomeres in the modified *synIX* strains split into two length groups; three groups of strains, yLHM1504 (containing the entire tRNA, intervening "gap" sequence between the tRNA and Ty1 with no known function, and Ty1 sequence), yLHM1506 (containing the tRNA and gap sequences but not the Ty1 sequence), and yLHM1601 (containing a tRNA with a transcription-inactivating point mutation[31–34] and the aforementioned gap sequence) had telomeres similar to or slightly longer than wild-type yeast, while two other groups of strains, yLHM1505 (containing just the gap sequence and Ty1 LTR) and yLHM1591 (containing just the gap), had telomeres shorter than BY4741 but slightly longer than yLHM1192. Thus, our experiments support the hypothesis posed but with a slight revision: we suggest that extension of telomeres beyond a crucial minimum threshold length suffices to restore fitness.

Next, we assessed the role of upstream *EST3* modifications on strain fitness and telomere length independent of other potential *synIX*-associated strain changes. We introduced each synthetic modification upstream of *EST3* (from yLHM1192, yLHM1504-1506, yLHM1591, and yLHM1601) into wild-type yeast (Figure 4A). As in *synIX* strains, yLHM1192-equivalent wild-type edited strains showed decreased fitness, but other modified strains showed normal fitness (Figure S9). Fitness did not change appreciably following extended strain passaging (Figure S9). As in the synthetic strains, we saw three groups of telomere lengths: wild type (BY4741, as well as the strains with the yLHM1504-, yLHM1506-, and yLHM1601-equivalent modifications), shortened (strains with the yLHM1192-equivalent modifications), and intermediate (strains with the yLHM1505- and yLHM1591-equivalent modifications) (Figure 4B).

We next sought to understand why all modifications improved fitness but only some fully restored telomere length to wild-type levels. We hypothesized that differences in *EST3* translation and/or transcription might result in variable telomere length across strains. To examine Est3p expression in modified *synIX* strains,

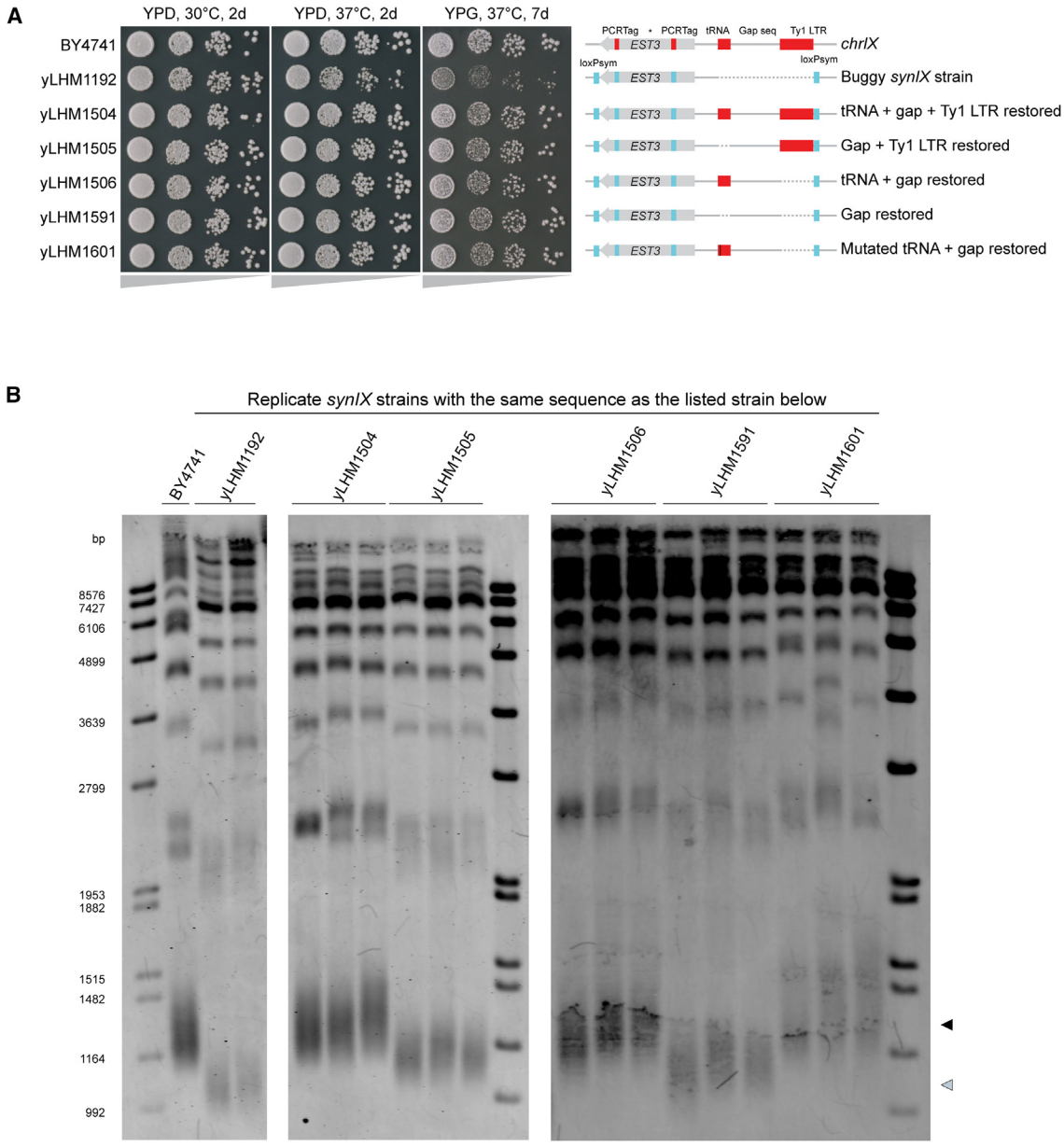

Figure 3. Modifying *synIX* strains upstream of *EST3* alters fitness and telomere length

(A) Spot assays and accompanying schematics of the region upstream of *EST3* for strains BY4741 (WT *chrIX*), yLHM1192 (synthetic), and variant strains derived from yLHM1192. WT PCRTags, $tRNA^{Asp}$ gene, and Ty1 LTR, red; synthetic PCRTags and loxPsym sites, blue; mutation in $tRNA^{Asp}$ gene, vertical black line. Each spot assay column represents a 10-fold dilution.

(B) Southern blot of *Xho*I-digested yeast gDNA derived from BY4741 (WT) and replicate strains with modifications equivalent to yLHM1192 (synthetic) and variant strains (yLHM1504, yLHM1505, yLHM1506, yLHM1591, and yLHM1601, as depicted in A). DNA was probed with a digoxigenin-labeled fragment specific for telomeric repeats. Black triangle (right): average size of Y′-containing telomeric fragments for BY4741. Gray triangle (right): average size of Y′-containing telomeric fragments for yLHM1192. Left and middle: left and right halves of one southern blot, cropped to remove one lane in the middle. Right: right side of second southern blot, cropped to remove left-hand ladder, BY4741, and yLHM1192 lanes.

See also Figure S8 and Table S6.

we tagged the 3′ end of *EST3* with 3× FLAG and evaluated protein levels at 37°C (Figure 5A; Table S7). FLAG-tagged synthetic strains were crossed to an untagged wild-type strain of opposite mating type (BY4742) to complement any potential recessive *synIX*-related effects on strain growth while allowing monitoring of *synIX*-derived Est3p levels. Consistent with telomere length data, yLHM1504-, yLHM1506-, and yLHM1601-derived strains expressed higher levels of FLAG-tagged Est3p than yLHM1192-, yLHM1505-, and yLHM1591-derived strains (Figure 5A). Follow-up comparisons of yLHM1192-, yLHM1505-, and

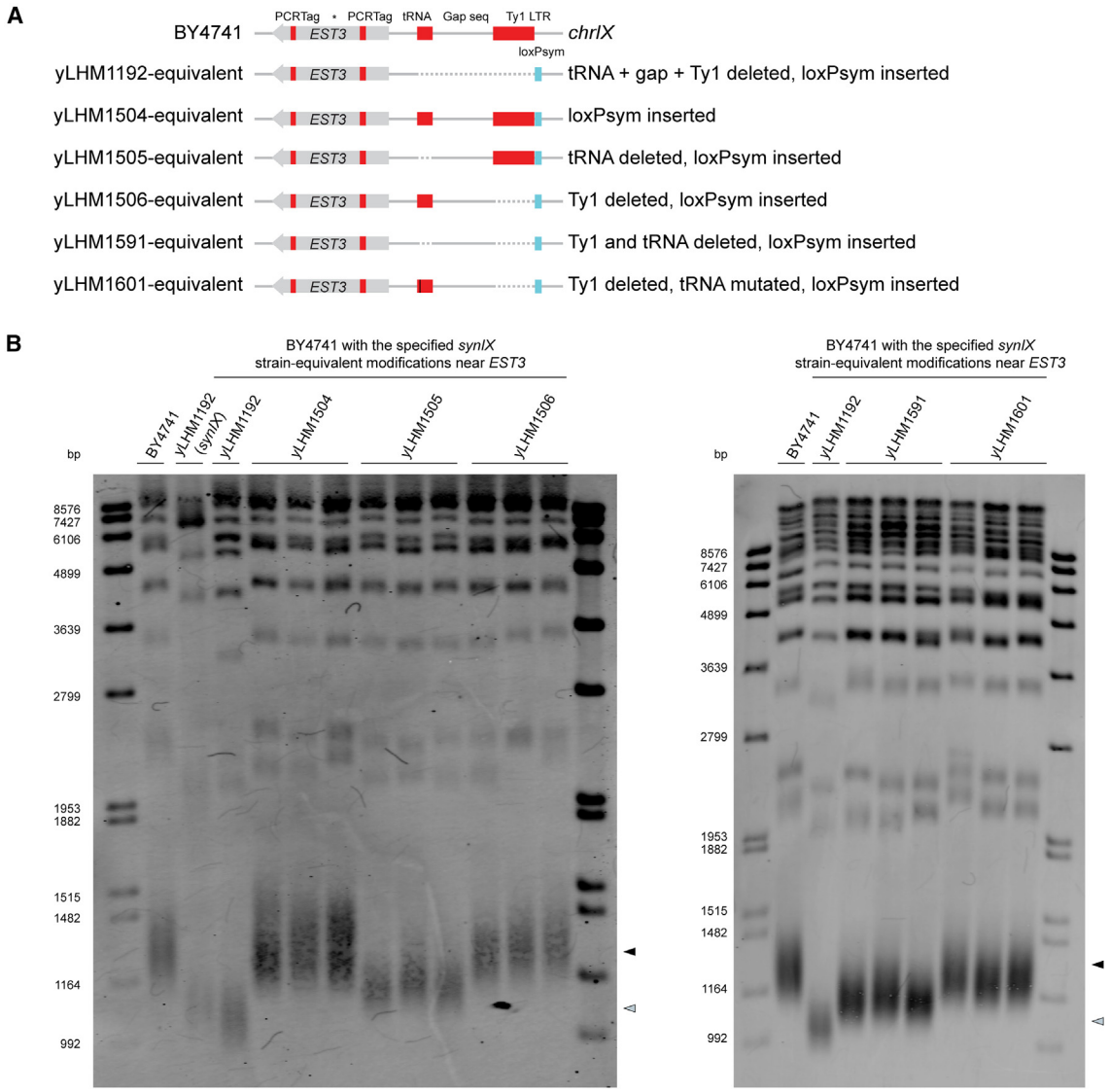

Figure 4. Modifying WT yeast strains upstream of *EST3* alters telomere length

(A) Schematics of region upstream of *EST3* for strains BY4741 (WT *chrIX*), yLHM1192-equivalent (synthetic modification matching yLHM1192 in otherwise WT yeast strain), and variant strains derived from the yLHM1192-equivalent strain. WT PCRTags, $tRNA^{Asp}$ gene, and Ty1 LTR, red; loxPsym sites, blue; mutation in $tRNA^{Asp}$ gene, vertical black line.

(B) Southern blot of *Xho*I-digested yeast gDNA derived from BY4741 (WT), yLHM1192 (synthetic), and replicate strains with synthetic-equivalent modifications made upstream of *EST3*, as depicted in (A). DNA was probed with a digoxigenin-labeled fragment specific for telomeric repeats. Black triangle (right): average size of Y′-containing telomeric fragments for BY4741. Gray triangle (right): average size of Y′-containing telomeric fragments for BY4741 + yLHM1192-equivalent modification strain.

See also Figure S9 and Table S6.

yLHM1591-derived strains revealed higher Est3p levels in yLHM1505- and yLHM1591-derived strains than in yLHM1192-derived strains, although all three strains had markedly lower Est3p levels than did FLAG-tagged wild-type yeast (Figure 5B). We saw neither longer nor shorter isoforms of FLAG-tagged Est3p associated with low-abundance strains (Figures 5B and S10). Similar results were observed in FLAG-tagged heterozygous diploid strains generated by crossing FLAG-tagged versions of the wild-type *EST3* variant strains from Figures 4A and S9 to untagged BY4742 and monitoring Est3p levels (Figures S11A and S11B). Collectively, the protein-level data support the hypothesis that Est3p levels were low and telomeres short in *synIX* strains, and modifications that increase telomere length appeared to do so by improving expression of Est3p. Moreover, a moderate level of Est3p gave rise to "medium"-length telomeres (longer than those in the *synIX* strain but shorter than those in wild-type strains), whereas higher (near-normal) levels of Est3p gave rise to longer telomeres. The $tRNA^{Asp}$ gene affected Est3p levels the most.

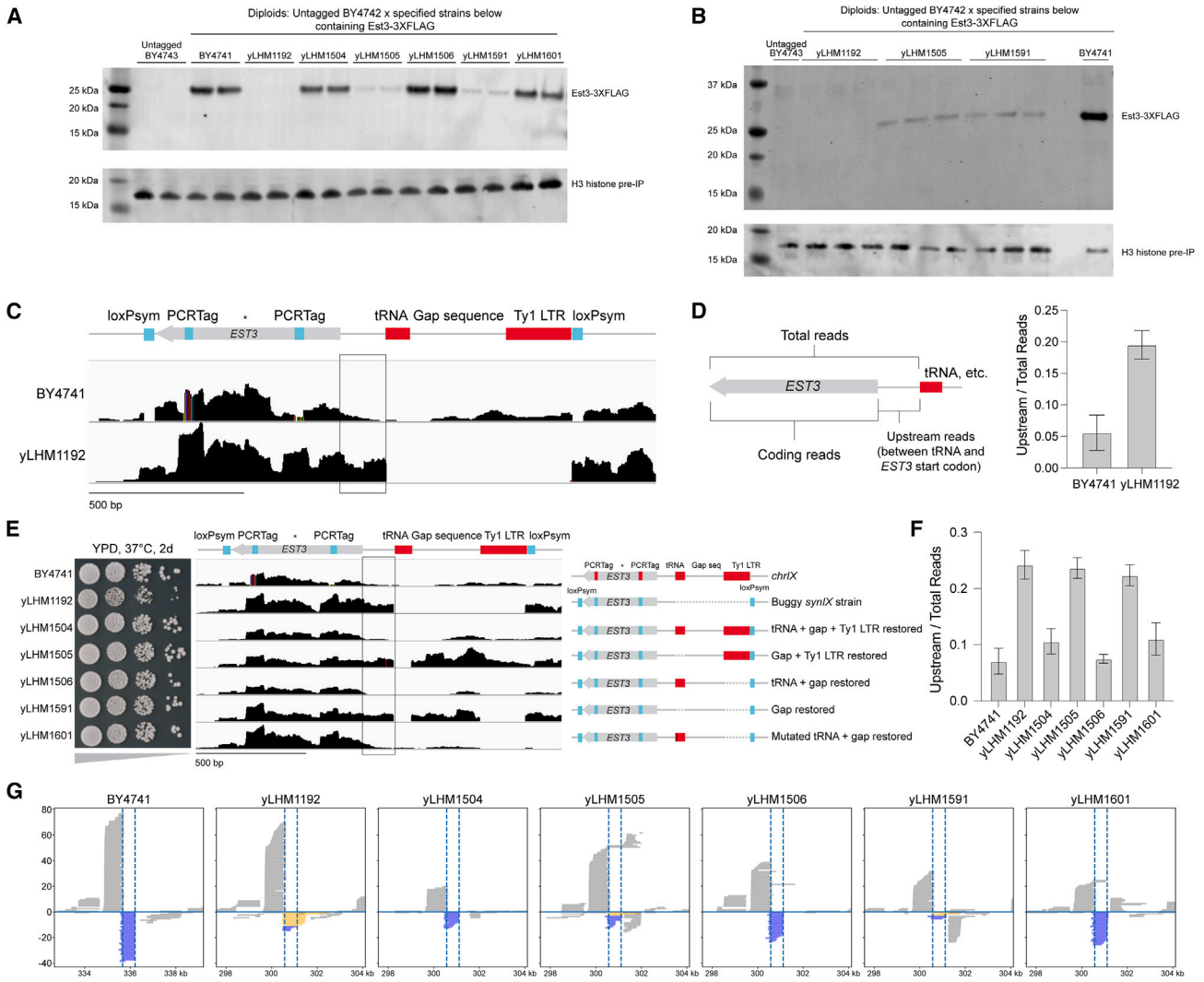

Figure 5. Dissecting effects of *EST3*-adjacent features on Est3 protein and *EST3* RNA expression

(A) Immunoblotting immunoprecipitated (IP/IB) Est3p (top) and H3 histone pre-IP loading control (bottom). Est3p was C-terminally tagged with 3× FLAG in each synthetic strain, and diploids were generated via mating with WT BY4742. Two independent colonies were grown in YPD at 37°C for each strain. Right-most lane (second ladder) was cropped out of image.

(B) IP/IB Est3p (top) and H3 histone pre-IP loading control (bottom) for low-expressing Est3p strains plus controls, as in (A), except that three independent colonies were grown for each yLHM1192-, yLHM1505-, and yLHM1591-derived diploid strain.

(C) Strand-specific RNA sequencing alignments for the reverse strand of BY4741 and yLHM1192 (strand from which *EST3* transcription is expected, i.e., "reverse-strand reads") grown at 37°C in YPD to a composite reference containing both synthetic and native *IX* features. Schematic illustrates WT *chrIX* (red) and synthetic (blue) features. Black box on RNA sequencing alignment plot highlights region between expected *EST3* start codon and upstream tRNA. Asterisk (*) marks site of known *EST3* programmed +1 ribosomal frameshift.

(D) Quantification of reverse-strand reads mapping directly upstream of *EST3* (between tRNA and start codon, corresponding to black box in C) as a fraction of total reverse-strand *EST3* coding and upstream reads for each strain shown in (C). Read counts were based on alignment to native (BY4741) or synthetic (yLHM1192) reference sequences. Error bars represent SD of three biological replicates.

(E) Spot assays and strand-specific RNA sequencing alignments for reverse-strand reads aligning to *EST3* region for samples grown at 37°C in YPD. WT PCRTags, $tRNA^{Asp}$ gene, and Ty1 LTR, red; synthetic PCRTags and loxPsym sites, blue; mutation in $tRNA^{Asp}$ gene, vertical black line. Asterisk (*) marks site of known *EST3* programmed +1 ribosomal frameshift.

(F) Quantification of reverse-strand reads mapping directly upstream of *EST3* (between tRNA and start codon, corresponding to black box in E) as fraction of total reverse-strand *EST3* coding and upstream reads for each strain shown in (E). Read counts were based on alignment to native (BY4741) or synthetic (yLHM1192) reference sequences. Error bars represent SD of three biological replicates.

(G) Nanopore direct RNA sequencing reads aligned to *EST3* region (±3 kb). The x axis: chromosome coordinate. The y axis: number of reads. Forward-strand reads are above the y axis, and reverse-strand reads are below the y axis. Dotted lines indicate boundaries of *EST3* coding region. Yellow reads:

(legend continued on next page)

To further elucidate what contributes to Est3p level variations in engineered *synIX* strains, we examined RNA sequencing data. Strand-specific RNA sequencing data revealed differences in the pattern of *EST3* transcripts in wild-type and *synIX* strains at 30°C and 37°C (Figures 5C, 5D, S12A, and S12B). In particular, while both strains showed sequencing read depth throughout the *EST3* coding region, *synIX* strains contained transcripts upstream of the expected *EST3* transcription start site (TSS) that were absent from BY4741. Importantly, since these transcripts were transcribed from the same strand as native *EST3*, some *EST3* transcripts might have had an extended 5′ UTR, predicted to encode upstream AUG codons that would not produce functional Est3p. In our modified *synIX* strains, we saw two classes of upstream transcript profiles (Figures 5E, 5F, S13A, and S13B). yLHM1504, yLHM1506, and yLHM1601, the three strains with wild-type-length or slightly longer telomeres, showed a relative reduction in RNA sequencing reads directly upstream of *EST3* compared with strand-specific total reads aligned to the upstream plus coding sequence of *EST3* (Figures 5E, 5F, S13A, and S13B). By contrast, yLHM1505 and yLHM1591, the two strains with intermediate-length telomeres, still showed substantial transcript read depth upstream of *EST3*. The wild-type strains with modifications upstream of *EST3* yielded similar transcriptional patterns (Figures S14A and S14B).

Nanopore direct RNA sequencing, which evaluates full-length transcript patterns, revealed a distinct population of *EST3*-spanning transcripts in yLHM1192 containing at least one out-of-frame AUG upstream of the expected *EST3* TSS (Figure 5G). Many of these transcripts started 250–500 bp upstream of the AUG that normally initiates Est3p translation (Figure S15). We hypothesize that such "nontranslatable" upstream transcripts fail to yield properly translated Est3p, contributing to reduced telomerase function and decreased strain fitness (Figure S16). By contrast, whereas yLHM1505 and yLHM1591 contained a few nontranslatable transcripts spanning *EST3*, most transcripts upstream of *EST3* observed in these strains terminated prior to the expected *EST3* TSS (gray in Figure 5G). yLHM1192, yLHM1505, and yLHM1591 all had relatively fewer full-length, presumably translatable *EST3* transcripts than did the tRNA-containing strains (yLHM1504, yLHM1506, and yLHM1601).

These results collectively point to a model in which upstream initiated transcripts normally "silenced" by the $tRNA^{Asp}$ are unable to produce Est3p and only reads initiating at or near the native TSS produce functional *EST3* transcripts and resulting protein. The original *synIX* strain (yLHM1192) appears to yield almost no functional Est3p, while variant strains produce either low (yLHM1505 and yLHM1591) or near-wild-type (yLHM1504, yLHM1506, and yLHM1601) Est3p levels. However, strains with even low levels of functional Est3p and moderate reduction in telomere length appear to surpass a threshold for maintaining normal strain fitness. Thus, three classes of Est3p abundance/telomere length yield only two fitness profiles: healthy and sick strains.

Characterization of the healthy *synIX* strain

We ultimately proceeded with the strain in which a mutated version of the deleted tRNA gene and the adjacent gap sequence were reintroduced upstream of *EST3* (yLHM1601 in Figure 5E). The tRNA sequence contained a point mutation previously shown to block tRNA transcription,[31–34] compatible with functional tRNA relocation to a tRNA neochromosome[15] while maintaining Est3p levels similar to those of wild-type yeast (Figure 5A). This strain is most consistent with Sc2.0's design principles of maximizing strain fitness while eliminating repetitive elements and tRNA genes. This final *synIX* version, coined yeast_chr09_9_2, grew similarly to wild-type yeast across a variety of media types and temperature conditions, as did additional sequence-matched replicate strains (Figures 6A and S17–S19). The final strain largely matched the expected synthetic reference sequence, with slight deviations from the original design reflecting changes made during bug fixing and other minor alterations during the assembly process (Table S8). The final strain also showed even coverage across *synIX* and normal chromosomal copy number (Figure 6B). *SynIX* migrated slightly faster on pulsed-field gel electrophoresis (PFGE) than did native *IX* (Figure 6C). We observed an unusual banding pattern among a couple of the higher bands in yLHM1601, possibly related to an expanded repetitive sequence near the telomere of *chrXVI*. This difference did not appear to affect strain fitness and disappeared following *synIX* transfer to an alternative matched-background wild-type yeast strain via the chromosome substitution method discussed in the next section (Figure 6C, lanes 3 and 4).

Transcriptional analysis of the final *synIX* strain (yLHM1601, or yeast_chr09_9_2) identified a small number of differentially expressed genes compared to the wild-type strain (Figures 6D, 6E, S20A, and S20B). Several hits found on *synIX* were located in or near telomeres, with some of these genes upregulated and others downregulated. On the left arm of *synIX*, *SOA1* (*YIL166C*) showed decreased expression in the *synIX* strain at 37°C (~5× lower than in BY4741). Several subtelomeric genes found between *SOA1* and *TEL09L* in native *chrIX* were deleted during *synIX* design. We hypothesize that *SOA1* expression decreased due to increased silencing associated with its new position near the left end UTC (universal telomere cap), as has been observed on other synthetic chromosomes where genes moved closer to UTCs due to subtelomeric DNA deletion.[12] Conversely, right-arm subtelomeric genes *YIR042C* and *YIR043C* showed expression increases at 37°C (~12× increase for *YIR042C*) and both 30°C and 37°C (~15× and ~34× increases for *YIR043C*), respectively. Unlike *SOA1*, *YIR042C* and *YIR043C* were already located very close to *TEL09R* in native *chrIX*. Consequently, the UTCs introduced to *synIX* per Sc2.0 design principles may have failed to silence nearby genes to

"nontranslatable" reads containing at least one AUG upstream of expected *EST3* start codon plus a minimum of 20 bp 5′ UTR sequence. Blue reads: reads mapping to *EST3* that start no more than 20 bp upstream of first AUG upstream of expected *EST3* start codon, including "translatable/functional" reads spanning the entirety of *EST3* and reads starting downstream of *EST3*-initiating AUG.
See also Figures S10–S16 and Tables S6–S7.

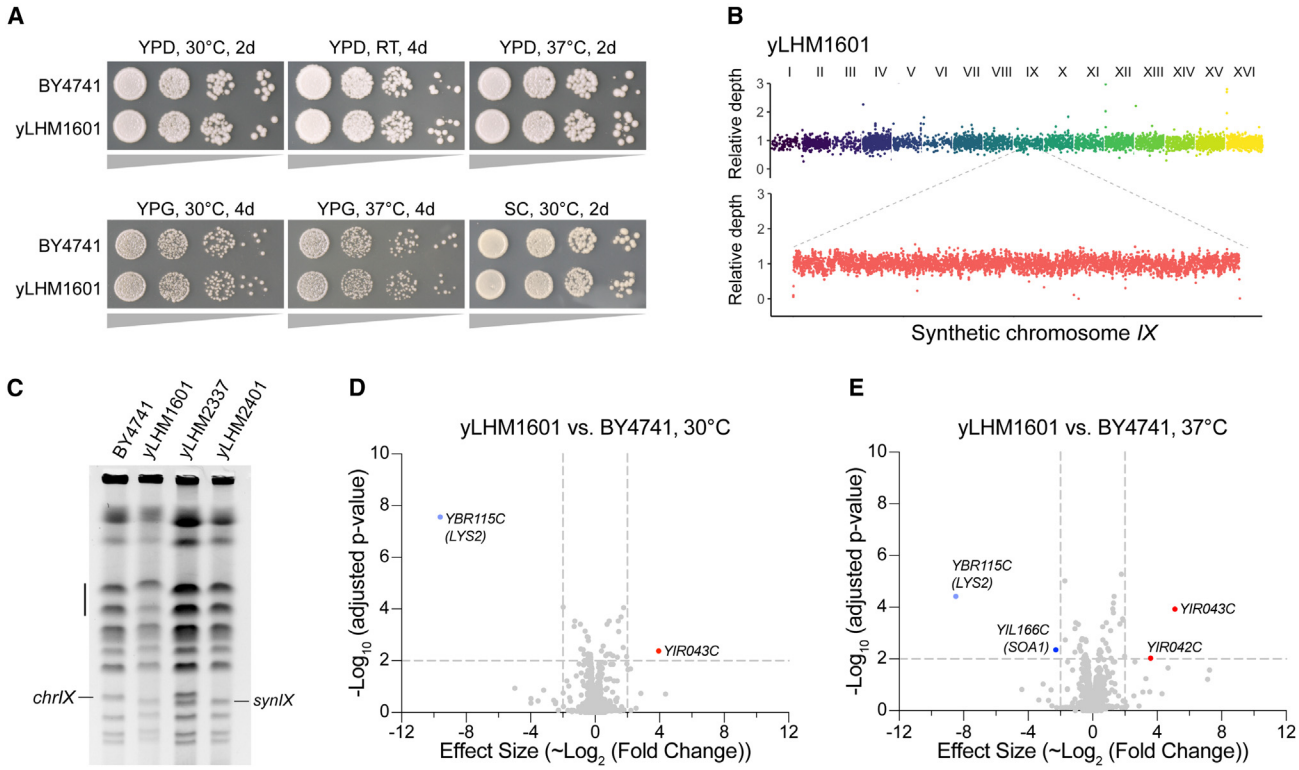

Figure 6. *SynIX* characterization

(A) Spot assays comparing growth of BY4741 (WT) to yLHM1601 (synthetic) across several conditions. Each column represents a 10-fold dilution. RT, room temperature, ~22°C.

(B) DNA sequencing coverage plot for *synIX* strain (yLHM1601). The x axis: yeast chromosome (not to scale) or coordinate along *synIX*. Relative depth (y axis) based on reads mapped to yeast_chr09_3_55 reference sequence divided by average read depth across sixteen yeast chromosomes (top) or *synIX* (bottom).

(C) Pulsed-field gel showing chromosomes from BY4741 (*chrIX*), yLHM1601 (*synIX*), yLHM2337 (BY4742-background strain with copies of *chrIX* and *synIX*), and yLHM2401 (yLHM2337 after loss of *chrIX*) strains. Vertical black line indicates location of potential discrepancy in band intensity for larger chromosomes between BY4741 and yLHM1601; *synIX* was moved to an alternative strain (yLHM2337) with larger bands resembling BY4741 in intensity, and *chrIX* was subsequently lost from this strain (producing yLHM2401) via strategy described in next section.

(D and E) Volcano plots of differentially expressed genes obtained from RNA sequencing data for *synIX* strain (yLHM1601) vs. BY4741 measured at 30°C (D) and 37°C (E) in YPD. Upregulated genes in yLHM1601 depicted in red (*chrIX*) and downregulated genes in medium blue (*chrIX*) or light blue (other chromosomes). Transcript counts based on alignment to S288C reference transcriptome. The auxotrophic gene *LYS2* is present in BY4741 but not in yLHM1601. Fold change cutoff is 4, and adjusted p value cutoff is 0.01. Three biological replicates were used for each strain. For corresponding unfiltered plots of RNA sequencing data depicting all measured genes, see Figures S20A and S20B.

See also Figures S17–S19 and Table S8.

the same degree as the native telomeres. Of note, the earliest version of the UTC, used at the right telomere, lacked the X sequence included at the left telomere and elsewhere in the Sc2.0 project. Since the X sequence is present in native *TEL09R,* its absence might help explain the selectively elevated expression of these *TEL09R*-adjacent genes.

Chromosome substitution of *synIX*

Here, we sought to combine chromoduction with subsequent loss of native *chrIX* from a recipient strain to seamlessly move *synIX* between yeast strains while maintaining normal karyotype in a strain of interest (Figure 7A). As a proof of concept, a disomic *synIX* strain was used as donor, as an extra copy of *synIX* was deemed likely to produce higher chromosome transfer efficiency.[25] A recipient *kar1-1* mutant strain blocked karyogamy. The recipient strain also contained two mutations, *can1* and *cyh2*, recessive selectable markers ensuring robust exclusion of donor cells and potential diploid cells on drug-containing medium. To facilitate selection for recipient strains containing *synIX* transferred from the donor, we deleted the *LYS12* gene in the recipient strain (Figure S21A). This allowed selection for lysine prototrophy to ensure *synIX*'s presence in the chromoductants. Additionally, to enable eventual loss of *chrIX* from the recipient, we subsequently knocked in a *URA3-pGAL* cassette upstream of *CEN9* in the recipient for *chrIX* destabilization and counterselection (Figure S21B).[27]

After modifying the recipient, we mated donor and recipient strains (yLHM0387 and yWZ601, respectively) and selected recipients that had acquired at least one copy of *synIX* via chromoduction on SC–Lys–Arg+Can+Cyh plates. A PCRTagging assay was performed using selected PCRTags across *chrIX* and *synIX*. Four chromoductants (yWZ610–613) containing both *chrIX* and

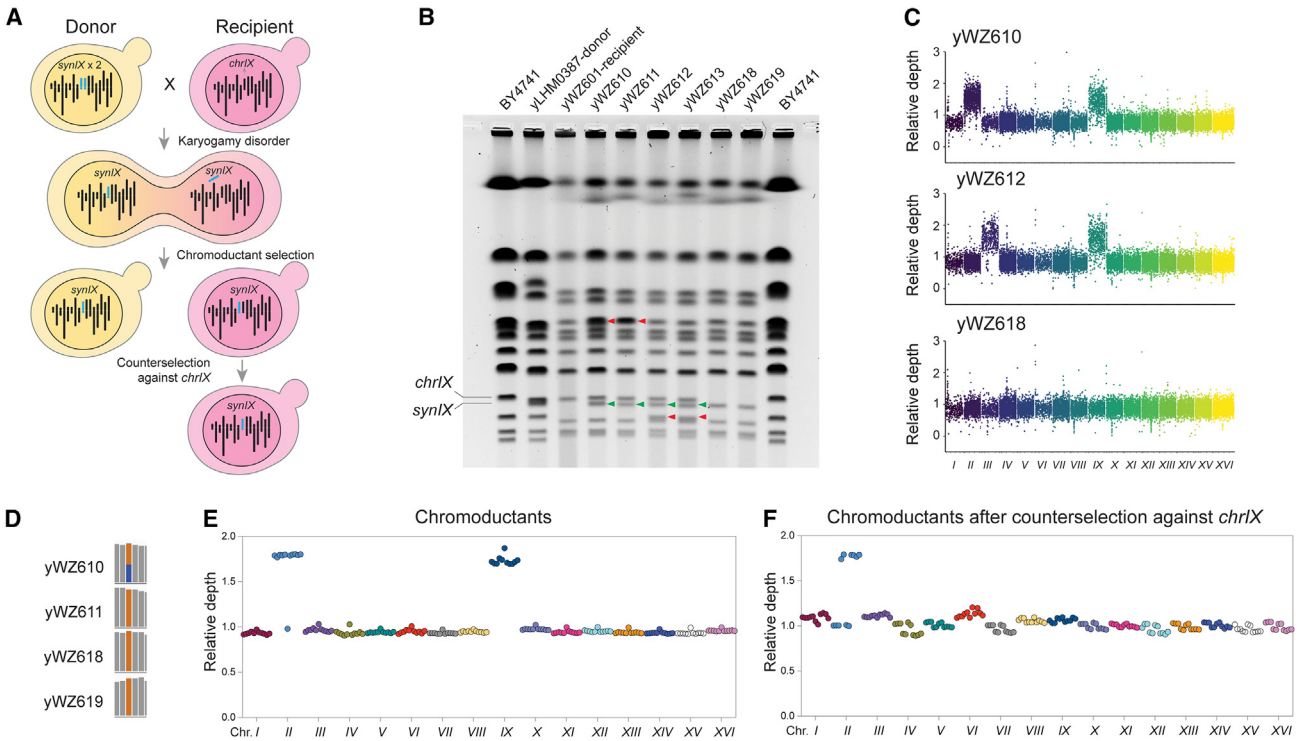

Figure 7. Chromosome substitution of *synIX*

(A) Chromosome substitution occurs in two steps, chromoduction, in which *synIX* is transferred to recipient strain, followed by counterselection against WT *chrIX* to remove native version of chromosome and restore normal chromosome copy number in chromoductant strain. Schematic diagram of substitution steps. Black bars, WT chromosomes. Blue bars, *synIX*. Recipient strain harbors an *ade2* mutation and thus forms pink colonies for easily distinguishing chromoductants.

(B) PFGE of donor strain, recipient strain, disomic chromoductants, and chromoductants after counterselection against *chrIX*. BY4741 serves as control. *chrIX* and *synIX* chromosomes indicated with black arrows. Green triangles indicate *synIX* in disomic chromoductants. Red triangles indicate extra *chrII* or *chrIII* in disomic chromoductants.

(C) Whole-genome sequencing read depth plots of disomic chromoductants (yWZ610, yWZ612) and *chrIX* counterselected (i.e., fully substituted) chromoductants (yWZ618). The x axis: sixteen yeast chromosomes, not drawn to scale. The y axis: relative read depth, calculated as number of reads at each position divided by average read depth across sixteen yeast chromosomes.

(D) *chrII* SNPs in chromoductant strains before and after counterselection against *chrIX*. Recipient strain SNP: orange, donor strain SNP: blue. Strains: yWZ610: chromoductant strain with one copy of *chrII* from donor strain and one from recipient strain (mixed SNP population); yWZ611: chromoductant strain with two copies of *chrII* from recipient strain (endoreduplicated *chrII*); yWZ618: strain derived from yWZ610 after counterselection against *chrIX*, with one copy of *chrII* harboring recipient strain SNP; yWZ619: strain derived from yWZ611 after counterselection against *chrIX*, with one copy of *chrII* harboring recipient strain SNP.

(E) Relative depth plot for chromosome substitution strains prior to counterselection against *chrIX*. The x axis: sixteen yeast chromosomes, not drawn to scale. The y axis: relative read depth.

(F) Relative depth plot for chromosome substitution strains after counterselection against *chrIX*. The x axis: sixteen yeast chromosomes, not drawn to scale. The y axis: relative read depth.

See also Figure S21 and Table S9.

synIX PCRTag amplicons were isolated from 14 candidates (Figure S21C). Disomic chromoductants stably maintained both *chrIX* and *synIX* upon restreaking onto SC–Lys plates. Genotyping validation of the four disomic chromoductants suggested that yWZ612 and yWZ613 had additionally acquired the *HIS4* gene on *chrIII* from the donor (the recipient was *his4Δ0*), suggesting that *chrIII* was co-transferred with *synIX* (Figure S21D).

To destabilize *chrIX* in the disomic chromoductants to generate haploids with a single copy of *synIX*, disomic chromoductants (yWZ610, yWZ611) were grown in galactose-containing medium to activate *GAL* transcription, destabilizing *CEN9* and consequently leading to *chrIX* loss.[27] PCRTagging analysis of the chromoductants (yWZ618, yWZ619) showed that only *synIX* was present (Figure S21E). PFGE analysis showed that (1) *synIX* was slightly smaller than *chrIX* in both BY4741 and the recipient strain; (2) both *synIX* and *chrIX* were present in disomic chromoductants; (3) *chrIII* was co-transferred with *synIX* in yWZ612 and yWZ613; and (4) *chrIX* was lost in chromoductants following counterselection against *chrIX* (yWZ618, yWZ619) (Figure 7B). However, two chromoductants, yWZ610 and yWZ611, surprisingly contained an extra copy of *chrII* in addition to both *chrIX* and *synIX* (Figure 7B), confirmed by whole-genome sequencing (Figure 7C). Further examination of SNPs differing between donor and recipient *chrII* revealed that yWZ610 contained one donor *chrII* and one recipient *chrII*, while yWZ611 contained two copies of recipient *chrII* (Figure 7D). This finding suggested that *chrII* endoreduplicated in yWZ611, perhaps to balance a gene dosage perturbation caused by *synIX*

chromoduction. Consistent with this hypothesis, one copy of *chrII* was lost from yWZ610 and yWZ611 during inactivation of *chrIX* (Figure 7B, yWZ618 and yWZ619).

To investigate whether co-transfer and simultaneous loss of *chrIX* and *chrII* was coincidental, we isolated 11 additional disomic chromoductants. Whole-genome sequencing revealed that 10 of the 11 disomic chromoductants gained an extra copy of *chrII* (Figure 7E). Following counterselection against *chrIX*, four disomic chromoductants lost *chrII*, while six chromoductants remained disomic (Figure 7F). To rule out that this was specific to our disomic *synIX* donor strain, we performed chromosome substitution using an alternative disomic *synIX* donor strain and three monosomic *synIX* donor strains. As in earlier experiments, *chrII* frequently co-transferred with *synIX*, and the extra copy of *chrII* often disappeared after culturing strains in galactose (Table S9). In conclusion, we successfully used chromosome substitution to transfer *synIX* from different donor strains to a *kar1-1* recipient strain via chromoduction and to subsequently destabilize *chrIX*. More in-depth diagnosis of chromoductants revealed that *chrII* was preferentially and consistently co-transferred with *synIX* and then frequently lost during counterselection against *chrIX*.

DISCUSSION

We successfully conclude the synthesis, debugging, and characterization of *synIX*. *synIX*'s complex developmental history reflects advances in DNA synthesis technology over more than a decade. When the project first began, each DNA segment was painstakingly assembled by undergraduates from oligonucleotides into minichunks, which in turn were integrated iteratively into the yeast genome to overwrite native *chrIX*. While such methods enabled successful incorporation of much of the synthetic sequence of interest, drawbacks included inadvertent retention of wild-type patches and introduction of new point mutations. Newer approaches, including direct minichunk synthesis and megachunk cloning and sequencing prior to integration, greatly improved assembly efficiency and reduced construction error rates. Ultimately, we produced a yeast strain with a fully synthetic version of *chrIX* displaying near-wild-type fitness.

While debugging *synIX*, we identified a fitness defect related to deletion of a DNA segment upstream of the *EST3* gene containing a $tRNA^{Asp}$ gene, a Ty1 LTR, and an intervening single-copy DNA sequence. Strains with this deletion showed a reduction in telomere length as well as reduced Est3p levels and many RNA species mapping upstream of *EST3*'s normal TSS. Reinserting all or part of the deleted sequence sufficed to restore normal fitness. However, only a subset of the edited strains, specifically those containing the tRNA gene, showed reduced transcriptional activity upstream of *EST3* and restoration of normal or near-normal Est3p levels and normal telomere length. We hypothesize that the tRNA sequence normally provides a buffer against production of aberrant transcripts upstream of *EST3*, and thus the transcripts that are produced in tRNA-containing strains more effectively give rise to functional, full-length Est3p. Indeed, tRNAs suppress transcription from nearby RNA polymerase II promoters in a process called tRNA-mediated gene silencing.[34–36] Consistent with this idea, nanopore RNA sequencing data suggests that a subset of transcripts include one or more AUGs upstream of *EST3* and thus presumably fail to undergo proper translation; strains with an abundance of such transcripts also appear to have fewer full-length, translatable transcripts and lower Est3p levels. Other changes made upstream of *EST3*, such as reinsertion of the gap sequence between the tRNA and the Ty1 LTR or Ty1 LTR itself, seemingly trigger small improvements in Est3p levels vs. those found in strains with the original *synIX* design. These strains have intermediate-length telomeres, longer than those seen in the original *synIX* design but shorter than those seen in native yeast, and maintain stable fitness after repeated passaging. We speculate that the changes introduced to these strains may be sufficient to maintain Est3p production and consequent telomere length above a threshold level needed for normal strain fitness, despite not fully returning either to native levels.

Interestingly, a similar occurrence of abnormal transcriptional patterns resulting from tRNA deletion and loxPsym site insertion was previously observed at the *HIS2* locus in *synVI*.[7] Here, the authors suggested that a "cryptic start site" upstream of *HIS2*, generated by the altered sequence in this region, might yield a subset of transcripts incapable of producing functional His2 protein or that this transcription might impair normal *HIS2* promoter activity. It would be useful to examine whether common principles underlie multiple Sc2.0 bugs following tRNA deletion.

Finally, we demonstrated a chromosome substitution technique that combines selective chromoduction, or movement of a desired chromosome between yeast strains, with subsequent destabilization and loss of the corresponding native chromosome. During this process of chromosome substitution, we found that certain chromosomes appeared to co-transfer with *synIX* at higher frequencies than did others. Specifically, we saw multiple instances of transfer of *chrII* or *chrIII* alongside *synIX*. These extra chromosomes often disappeared following destabilization of *chrIX*. Prior work suggested that smaller chromosomes are more likely to transfer during chromoduction than larger ones and that co-transfer of multiple chromosomes commonly occurs.[24] However, as *chrII* is not small, it seems unlikely that chromosome size fully explains specific *chrII* co-transfer.

It is likely that an extra copy of *chrII* compensates for a gene dosage imbalance arising from the transient extra copy of *chrIX* introduced by chromoduction. In one chromoductant strain, analysis of SNPs from the recipient and donor strains' copies of *chrII* revealed that both copies of the chromosome came from the recipient strain. The presence of an endoreduplicated *chrII* is consistent with the hypothesis that there is selective pressure for a higher dosage of *chrII* fitness in the presence of two copies of *chrIX* and that co-migration of *chrII* and *synIX* in the other chromoductant strains may not have occurred by chance. Moreover, multiple donor strains, including strains disomic and monosomic for *synIX*, showed co-transfer of *chrII* alongside *synIX*. It may be informative to ascertain mechanisms that dictate which chromosomes tend to show such co-chromoduction.

Ultimately, chromosome substitution has numerous applications, including transfer and consolidation of chromosomes

from other wild-type yeast strains, engineered strains, and non-laboratory strains. Existing work profiling collections of hundreds or thousands of yeast strains has shed light on yeast diversity and evolution[37–39]; chromosome substitution will facilitate further probing of how changes on individual chromosomes or combinations of chromosomes affect strain fitness and function. Similarly, this technology could assist in analyzing why genomic changes in SCRaMbLEd yeast strains and other engineered strains produce particular phenotypic results.[1–4] More immediately, chromosome substitution is already in use to bring the initial phase of Sc2.0 to a close via consolidation of all of the synthetic chromosomes into a single strain, marking a key eukaryotic genome engineering milestone.[22]

Limitations of the study

SynIX is but one of sixteen synthetic yeast chromosomes assembled as part of Sc2.0. Consequently, the efforts made here are limited compared to what can be done following chromosome consolidation of most or all synthetic chromosomes into a single yeast strain. The chromosome substitution method described here will facilitate generation of such consolidated chromosome strains for further study. Additionally, our analysis of the *EST3* bug could be made even more comprehensive by making additional variants of the region upstream of that gene and testing those modifications in additional backgrounds.

CONSORTIA

This work is part of the international Synthetic Yeast Genome (Sc2.0) consortium. The chromosome design and building consortium includes research groups worldwide: Boeke Lab at Johns Hopkins University and New York University (led chromosomes I, III, IV, VI, VIII, IX); Chandrasegaran lab at Johns Hopkins (led chromosomes III and IX); Cai Lab at University of Edinburgh and University of Manchester (led chromosomes II and VII and tRNA neochromosome); Yue Shen's team at BGI-Research SHENZHEN (led chromosomes II, VII, and XIII); Y.J. Yuan's team at Tianjin University (led chromosomes V and X); Dai Lab at Tsinghua University and Shenzhen Institute of Advanced Technology, CAS (led chromosome XII); Ellis Lab at Imperial College London (led chromosome XI); Sakkie Pretorius's team at Macquarie University (led chromosomes XIV and XVI); Matthew Wook Chang's team at National University of Singapore (led chromosome XV); Bader and Boeke Labs at Johns Hopkins University (led design and workflow); and Build-A-Genome undergraduate teams at Johns Hopkins University and Loyola University Maryland (contributed to chromosomes I, III, IV, VIII, and IX). The Sc2.0 consortium includes numerous other participants who are acknowledged on the project website, www.syntheticyeast.org.

STAR★METHODS

Detailed methods are provided in the online version of this paper and include the following:

SUPPLEMENTAL INFORMATION

Supplemental information can be found online at https://doi.org/10.1016/j.xgen.2023.100419.

ACKNOWLEDGMENTS

We thank Meghan O'Keefe for collecting the BAG student authors' information. The work reported here forms a portion of L.H.M.'s PhD thesis. We thank the NSF for grants MCB-1026068, MCB-1443299, MCB-1616111, and MCB-1921641 to J.D.B. and MCB-1445545 to J.S.B., which support this work.

AUTHOR CONTRIBUTIONS

J.D.B., S.C., and W.Z. conceptualized the study. W.Z., S.C., L.H.M., and J.D.B. designed the experiments. J.D.B. and J.S.B. designed *synIX*. The Build-A-Genome class members constructed building blocks. V.S., N.A., and S.R. constructed minichunks and incorporated them for megachunks A–F. L.H.M. designed, constructed, and delivered megachunks G–I and performed error correction, bug mapping, bug correction, and functional studies of *synIX*. L.H.M. and W.Z. developed and evaluated the chromosome substitution method. L.H.M., A.L.H., J.C., V.F., E.L., and G.S. performed sequencing and data analyses. L.H.M., W.Z., and J.D.B. wrote the manuscript. L.A.M., H.J., J.L., M.S.T., and W.R.B. provided advice. S.C., J.D.B., J.S.B., and L.M.S. provided lab supervision. All authors reviewed and edited the manuscript.

DECLARATION OF INTERESTS

J.D.B. is a founder and director of CDI Labs, Inc., a founder of and consultant to Neochromosome, Inc, a founder, SAB member of, and consultant to ReOpen Diagnostics, LLC, and serves or served on the scientific advisory board of the following: Logomix, Inc., Sangamo, Inc., Modern Meadow, Inc., Rome Therapeutics, Inc., Sample6, Inc., Tessera Therapeutics, Inc., and the Wyss Institute. J.S.B. is a founder of Neochromosome, Inc., consultant to Opentrons Labworks, Inc., and advisor to Reflexion Pharmaceuticals, Inc.

Received: October 26, 2022
Revised: September 7, 2023
Accepted: September 11, 2023
Published: November 8, 2023

REFERENCES

1. Dymond, J., and Boeke, J. (2012). The Saccharomyces cerevisiae SCRaMbLE system and genome minimization. Bioeng. Bugs *3*, 168–171. https://doi.org/10.4161/bbug.19543.
2. Richardson, S.M., Mitchell, L.A., Stracquadanio, G., Yang, K., Dymond, J.S., DiCarlo, J.E., Lee, D., Huang, C.L.V., Chandrasegaran, S., Cai, Y., et al. (2017). Design of a synthetic yeast genome. Science *355*, 1040–1044. https://doi.org/10.1126/science.aaf4557.
3. Shen, M.J., Wu, Y., Yang, K., Li, Y., Xu, H., Zhang, H., Li, B.Z., Li, X., Xiao, W.H., Zhou, X., et al. (2018). Heterozygous diploid and interspecies SCRaMbLEing. Nat. Commun. *9*, 1934. https://doi.org/10.1038/s41467-018-04157-0.
4. Shen, Y., Stracquadanio, G., Wang, Y., Yang, K., Mitchell, L.A., Xue, Y., Cai, Y., Chen, T., Dymond, J.S., Kang, K., et al. (2016). SCRaMbLE generates designed combinatorial stochastic diversity in synthetic chromosomes. Genome Res. *26*, 36–49. https://doi.org/10.1101/gr.193433.115.
5. Annaluru, N., Muller, H., Mitchell, L.A., Ramalingam, S., Stracquadanio, G., Richardson, S.M., Dymond, J.S., Kuang, Z., Scheifele, L.Z., Cooper, E.M., et al. (2014). Total synthesis of a functional designer eukaryotic chromosome. Science *344*, 55–58. https://doi.org/10.1126/science.1249252.
6. Dymond, J.S., Richardson, S.M., Coombes, C.E., Babatz, T., Muller, H., Annaluru, N., Blake, W.J., Schwerzmann, J.W., Dai, J., Lindstrom, D.L., et al. (2011). Synthetic chromosome arms function in yeast and generate phenotypic diversity by design. Nature *477*, 471–476. https://doi.org/10.1038/nature10403.
7. Mitchell, L.A., Wang, A., Stracquadanio, G., Kuang, Z., Wang, X., Yang, K., Richardson, S., Martin, J.A., Zhao, Y., Walker, R., et al. (2017). Synthesis, debugging, and effects of synthetic chromosome consolidation: synVI and beyond. Science *355*, eaaf4831. https://doi.org/10.1126/science.aaf4831.
8. Shen, Y., Wang, Y., Chen, T., Gao, F., Gong, J., Abramczyk, D., Walker, R., Zhao, H., Chen, S., Liu, W., et al. (2017). Deep functional analysis of synII, a 770-kilobase synthetic yeast chromosome. Science *355*, eaaf4791. https://doi.org/10.1126/science.aaf4791.
9. Wu, Y., Li, B.Z., Zhao, M., Mitchell, L.A., Xie, Z.X., Lin, Q.H., Wang, X., Xiao, W.H., Wang, Y., Zhou, X., et al. (2017). Bug mapping and fitness testing of chemically synthesized chromosome X. Science *355*, eaaf4706. https://doi.org/10.1126/science.aaf4706.
10. Xie, Z.X., Li, B.Z., Mitchell, L.A., Wu, Y., Qi, X., Jin, Z., Jia, B., Wang, X., Zeng, B.X., Liu, H.M., et al. (2017). Perfect" designer chromosome V and behavior of a ring derivative. Science *355*, eaaf4704. https://doi.org/10.1126/science.aaf4704.
11. Zhang, W., Zhao, G., Luo, Z., Lin, Y., Wang, L., Guo, Y., Wang, A., Jiang, S., Jiang, Q., Gong, J., et al. (2017). Engineering the ribosomal DNA in a megabase synthetic chromosome. Science *355*, eaaf3981. https://doi.org/10.1126/science.aaf3981.
12. Zhang, W., Lazar-Stefanita, L., Yamashita, H., Shen, M.J., Mitchell, L.A., Kurasawa, H., Haase, M.A.B., Sun, X., Jiang, Q., Lauer, S.L., et al. (2022). Manipulating the 3D Organization of the Largest Synthetic Yeast Chromosome, 2022.2004.2009.487066. https://doi.org/10.1101/2022.04.09.487066 %J bioRxiv.
13. Blount, B.A., Lu, X., Driessen, M.R.M., Jovicevic, D., Sanchez, M.I., Ciurkot, K., Zhao, Y., Lauer, S., McKiernan, R.M., Gowers, G.-O.F., et al. (2022). Synthetic Yeast Chromosome XI Design Enables Extrachromosomal Circular DNA Formation on Demand, 2022.2007.2015.500197. https://doi.org/10.1101/2022.07.15.500197 %J bioRxiv.
14. Williams, T.C., Kroukamp, H., Xu, X., Wightman, E.L.I., Llorente, B., Borneman, A.R., Carpenter, A.C., Van Wyk, N., Espinosa, M.I., Daniel, E.L., et al. (2022). Laboratory Evolution and Polyploid SCRaMbLE Reveal Genomic Plasticity to Synthetic Chromosome Defects and Rearrangements, 2022.2007.2022.501046. https://doi.org/10.1101/2022.07.22.501046 %J bioRxiv.
15. Schindler, D., Walker, R.S.K., Jiang, S., Brooks, A.N., Wang, Y., Müller, C.A., Cockram, C., Luo, Y., García, A., Schraivogel, D., et al. (2022). Design, Construction, and Functional Characterization of a tRNA Neochromosome in Yeast, 2022.2010.2003.510608. https://doi.org/10.1101/2022.10.03.510608 %J bioRxiv.
16. Shen, Y., Gao, F., Wang, Y., Wang, Y., Zheng, J., Gong, J., Zhang, J., Luo, Z., Schindler, D., Deng, Y., et al. (2022). Dissecting Aneuploidy Phenotypes by Constructing Sc2.0 Chromosome VII and SCRaMbLEing Synthetic Disomic Yeast, 2022.2009.2001.506252. https://doi.org/10.1101/2022.09.01.506252 %J bioRxiv.
17. Luo, J., Mercy, G., Vale-Silva, L.A., Sun, X., Agmon, N., Zhang, W., Yang, K., Stracquadanio, G., Thierry, A., Ahn, J.Y., et al. (2018). Synthetic Chromosome Fusion: Effects on Genome Structure and Function, 381137. https://doi.org/10.1101/381137 %J bioRxiv.
18. Lauer, S., Luo, J., Lazar-Stefanita, L., Zhang, W., McCulloch, L.H., Fanfani, V., Lobzaev, E., Haase, M.A.B., Easo, N., Zhao, Y., et al. (2023). Context-dependent neocentromere activity in synthetic yeast chromosome VIII. Cell Genomics. in revision.
19. Lendvay, T.S., Morris, D.K., Sah, J., Balasubramanian, B., and Lundblad, V. (1996). Senescence mutants of Saccharomyces cerevisiae with a defect in telomere replication identify three additional EST genes. Genetics *144*, 1399–1412. https://doi.org/10.1093/genetics/144.4.1399.
20. Morris, D.K., and Lundblad, V. (1997). Programmed translational frameshifting in a gene required for yeast telomere replication. Curr. Biol. *7*, 969–976. https://doi.org/10.1016/s0960-9822(06)00416-7.
21. Hughes, T.R., Evans, S.K., Weilbaecher, R.G., and Lundblad, V. (2000). The Est3 protein is a subunit of yeast telomerase. Curr. Biol. *10*, 809–812. https://doi.org/10.1016/s0960-9822(00)00562-5.
22. Zhao, Y., Coelho, C., Hughes, A.L., Lazar-Stefanita, L., Yang, S., Brooks, A.N., Walker, R.S.K., Zhang, W., Lauer, S., Hernandez, C., et al. (2022). Debugging and Consolidating Multiple Synthetic Chromosomes Reveals Combinatorial Genetic Interactions, 2022.2004.2011.486913. https://doi.org/10.1101/2022.04.11.486913 %J bioRxiv.
23. Conde, J., and Fink, G.R. (1976). A mutant of Saccharomyces cerevisiae defective for nuclear fusion. Proc. Natl. Acad. Sci. USA *73*, 3651–3655. https://doi.org/10.1073/pnas.73.10.3651.
24. Dutcher, S.K. (1981). Internuclear transfer of genetic information in kar1-1/KAR1 heterokaryons in Saccharomyces cerevisiae. Mol. Cell Biol. *1*, 245–253. https://doi.org/10.1128/mcb.1.3.245-253.1981.
25. Ji, H., Moore, D.P., Blomberg, M.A., Braiterman, L.T., Voytas, D.F., Natsoulis, G., and Boeke, J.D. (1993). Hotspots for unselected Ty1 transposition events on yeast chromosome III are near tRNA genes and LTR sequences. Cell *73*, 1007–1018. https://doi.org/10.1016/0092-8674(93)90278-x.
26. Guo, Z., Yin, H., Ma, L., Li, J., Ma, J., Wu, Y., and Yuan, Y. (2022). Direct Transfer and Consolidation of Synthetic Yeast Chromosomes by Abortive Mating and Chromosome Elimination. ACS Synth. Biol. *11*, 3264–3272. https://doi.org/10.1021/acssynbio.2c00174.

27. Reid, R.J.D., Sunjevaric, I., Voth, W.P., Ciccone, S., Du, W., Olsen, A.E., Stillman, D.J., and Rothstein, R. (2008). Chromosome-scale genetic mapping using a set of 16 conditionally stable Saccharomyces cerevisiae chromosomes. Genetics *180*, 1799–1808. https://doi.org/10.1534/genetics.108.087999.

28. Johnson, D.R., Knoll, L.J., Levin, D.E., and Gordon, J.I. (1994). Saccharomyces cerevisiae contains four fatty acid activation (FAA) genes: an assessment of their role in regulating protein N-myristoylation and cellular lipid metabolism. J. Cell Biol. *127*, 751–762. https://doi.org/10.1083/jcb.127.3.751.

29. Knoll, L.J., Johnson, D.R., and Gordon, J.I. (1994). Biochemical studies of three Saccharomyces cerevisiae acyl-CoA synthetases, Faa1p, Faa2p, and Faa3p. J. Biol. Chem. *269*, 16348–16356.

30. Yoshikawa, K., Tanaka, T., Ida, Y., Furusawa, C., Hirasawa, T., and Shimizu, H. (2011). Comprehensive phenotypic analysis of single-gene deletion and overexpression strains of Saccharomyces cerevisiae. Yeast *28*, 349–361. https://doi.org/10.1002/yea.1843.

31. Devine, S.E., and Boeke, J.D. (1996). Integration of the yeast retrotransposon Ty1 is targeted to regions upstream of genes transcribed by RNA polymerase III. Genes Dev. *10*, 620–633. https://doi.org/10.1101/gad.10.5.620.

32. Geiduschek, E.P., and Tocchini-Valentini, G.P. (1988). Transcription by RNA polymerase III. Annu. Rev. Biochem. *57*, 873–914. https://doi.org/10.1146/annurev.bi.57.070188.004301.

33. Newman, A.J., Ogden, R.C., and Abelson, J. (1983). tRNA gene transcription in yeast: effects of specified base substitutions in the intragenic promoter. Cell *35*, 117–125. https://doi.org/10.1016/0092-8674(83)90214-3.

34. Hull, M.W., Erickson, J., Johnston, M., and Engelke, D.R. (1994). tRNA genes as transcriptional repressor elements. Mol. Cell Biol. *14*, 1266–1277. https://doi.org/10.1128/mcb.14.2.1266-1277.1994.

35. Bolton, E.C., and Boeke, J.D. (2003). Transcriptional interactions between yeast tRNA genes, flanking genes and Ty elements: a genomic point of view. Genome Res. *13*, 254–263. https://doi.org/10.1101/gr.612203.

36. Donze, D. (2012). Extra-transcriptional functions of RNA Polymerase III complexes: TFIIIC as a potential global chromatin bookmark. Gene *493*, 169–175. https://doi.org/10.1016/j.gene.2011.09.018.

37. Peter, J., De Chiara, M., Friedrich, A., Yue, J.X., Pflieger, D., Bergström, A., Sigwalt, A., Barre, B., Freel, K., Llored, A., et al. (2018). Genome evolution across 1,011 Saccharomyces cerevisiae isolates. Nature *556*, 339–344. https://doi.org/10.1038/s41586-018-0030-5.

38. Liti, G., Carter, D.M., Moses, A.M., Warringer, J., Parts, L., James, S.A., Davey, R.P., Roberts, I.N., Burt, A., Koufopanou, V., et al. (2009). Population genomics of domestic and wild yeasts. Nature *458*, 337–341. https://doi.org/10.1038/nature07743.

39. Strope, P.K., Skelly, D.A., Kozmin, S.G., Mahadevan, G., Stone, E.A., Magwene, P.M., Dietrich, F.S., and McCusker, J.H. (2015). The 100-genomes strains, an S. cerevisiae resource that illuminates its natural phenotypic and genotypic variation and emergence as an opportunistic pathogen. Genome Res. *25*, 762–774. https://doi.org/10.1101/gr.185538.114.

40. Richardson, S.M., Wheelan, S.J., Yarrington, R.M., and Boeke, J.D. (2006). GeneDesign: rapid, automated design of multikilobase synthetic genes. Genome Res. *16*, 550–556. https://doi.org/10.1101/gr.4431306.

41. Robinson, J.T., Thorvaldsdóttir, H., Winckler, W., Guttman, M., Lander, E.S., Getz, G., and Mesirov, J.P. (2011). Integrative genomics viewer. Nat. Biotechnol. *29*, 24–26. https://doi.org/10.1038/nbt.1754.

42. Bolger, A.M., Lohse, M., and Usadel, B. (2014). Trimmomatic: a flexible trimmer for Illumina sequence data. Bioinformatics *30*, 2114–2120. https://doi.org/10.1093/bioinformatics/btu170.

43. Andrews, S. (2010). FastQC: A Quality Control Tool for High Throughput Sequence Data. http://www.bioinformatics.babraham.ac.uk/projects/fastqc/.

44. Langmead, B., and Salzberg, S.L. (2012). Fast gapped-read alignment with Bowtie 2. Nat. Methods *9*, 357–359. https://doi.org/10.1038/nmeth.1923.

45. Wickham, H. (2016). ggplot2: Elegant Graphics for Data Analysis (Springer-Verlag).

46. Bray, N.L., Pimentel, H., Melsted, P., and Pachter, L. (2016). Near-optimal probabilistic RNA-seq quantification. Nat. Biotechnol. *34*, 525–527. https://doi.org/10.1038/nbt.3519.

47. Dobin, A., Davis, C.A., Schlesinger, F., Drenkow, J., Zaleski, C., Jha, S., Batut, P., Chaisson, M., and Gingeras, T.R. (2013). STAR: ultrafast universal RNA-seq aligner. Bioinformatics *29*, 15–21. https://doi.org/10.1093/bioinformatics/bts635.

48. Li, H., Handsaker, B., Wysoker, A., Fennell, T., Ruan, J., Homer, N., Marth, G., Abecasis, G., and Durbin, R.; 1000 Genome Project Data Processing Subgroup (2009). The Sequence Alignment/Map format and SAMtools. Bioinformatics *25*, 2078–2079. https://doi.org/10.1093/bioinformatics/btp352.

49. Quinlan, A.R., and Hall, I.M. (2010). BEDTools: a flexible suite of utilities for comparing genomic features. Bioinformatics *26*, 841–842. https://doi.org/10.1093/bioinformatics/btq033.

50. Pimentel, H., Bray, N.L., Puente, S., Melsted, P., and Pachter, L. (2017). Differential analysis of RNA-seq incorporating quantification uncertainty. Nat. Methods *14*, 687–690. https://doi.org/10.1038/nmeth.4324.

51. Brachmann, C.B., Davies, A., Cost, G.J., Caputo, E., Li, J., Hieter, P., and Boeke, J.D. (1998). Designer deletion strains derived from Saccharomyces cerevisiae S288C: a useful set of strains and plasmids for PCR-mediated gene disruption and other applications. Yeast *14*, 115–132. https://doi.org/10.1002/(SICI)1097-0061(19980130)14:2<115::AID-YEA204>3.0.CO;2-2.

52. DiCarlo, J.E., Norville, J.E., Mali, P., Rios, X., Aach, J., and Church, G.M. (2013). Genome engineering in Saccharomyces cerevisiae using CRISPR-Cas systems. Nucleic Acids Res. *41*, 4336–4343. https://doi.org/10.1093/nar/gkt135.

53. Litovchick, L. (2020). Immunoblotting. Cold Spring Harb. Protoc. *2020*, 098392. https://doi.org/10.1101/pdb.top098392.

54. Brooks, A.N., Hughes, A.L., Clauder-Münster, S., Mitchell, L.A., Boeke, J.D., and Steinmetz, L.M. (2022). Transcriptional neighborhoods regulate transcript isoform lengths and expression levels. Science *375*, 1000–1005. https://doi.org/10.1126/science.abg0162.

55. Domanski, M., Molloy, K., Jiang, H., Chait, B.T., Rout, M.P., Jensen, T.H., and LaCava, J. (2012). Improved methodology for the affinity isolation of human protein complexes expressed at near endogenous levels. Biotechniques *0*, 1–6. https://doi.org/10.2144/000113864.

56. Luo, J., Sun, X., Cormack, B.P., and Boeke, J.D. (2018). Karyotype engineering by chromosome fusion leads to reproductive isolation in yeast. Nature *560*, 392–396. https://doi.org/10.1038/s41586-018-0374-x.

STAR★METHODS

KEY RESOURCES TABLE

REAGENT or RESOURCE	SOURCE	IDENTIFIER
Antibodies		
Digoxigenin Recombinant Rabbit Monoclonal Antibody (9H27L19)	Invitrogen	Thermo Fisher Scientific Cat# 700772; RRID:AB_2532342
Monoclonal ANTI-FLAG® M2 antibody produced in mouse	Sigma-Aldrich	Sigma-Aldrich Cat# F1804; RRID:AB_262044
Rabbit anti-Histone H3 antibody	Abcam	Abcam Cat# ab1791; RRID:AB_302613
IRDye 800CW Goat anti-Mouse IgG1-Specific	LI-COR Biosciences	LI-COR Biosciences Cat# 926–32350; RRID:AB_2782997
IRDye 680RD Goat anti-Rabbit IgG	LI-COR Biosciences	LI-COR Biosciences Cat# 926–68071; RRID:AB_10956166
Bacterial and virus strains		
EPI300 *E. coli* strain	Lucigen	EC300150
TOP10 *E coli* strain	Invitrogen	C4040
Chemicals, peptides, and recombinant proteins		
Zymolyase 20T	US Biological	Z1000
Zymolyase 100T	US Biological	Z1004
EDTA-free protease inhibitor	Roche	11873580001
Lithium acetate dihydrate	Sigma-Aldrich	L6883
Polyethylene glycol	Sigma-Aldrich	81188
Herring sperm DNA	Promega	D1816
Potassium acetate	Fisher	BP364
Zinc acetate dihydrate	Sigma-Aldrich	Z0625
(S)-(+)-Camptothecin	Sigma-Aldrich	C9911
D-Sorbitol	Sigma-Aldrich	S1876
6-Azauracil	Sigma-Aldrich	A1757
Hydroxyurea	Sigma-Aldrich	H8627
Methyl methanesulfonate	Sigma-Aldrich	129925
Methyl 1-(butylcarbamoyl)-2-benzimidazolecarbamate (Benomyl)	Sigma-Aldrich	381586
Cycloheximide	Sigma-Aldrich	01810
L-Canavanine sulfate	Sigma-Aldrich	C9758
Hydrogen peroxide	Millipore	88597
ULTRAhyb™ Ultrasensitive Hybridization Buffer	Invitrogen	AM8669
SSPE Buffer 20X Concentrate	Sigma-Aldrich	S2015
Intercept (TBS) Blocking Buffer	LI-COR Biosciences	927–60001
TWEEN 20	Sigma-Aldrich	P1379
Triton™ X-100	Sigma-Aldrich	X100
2-Mercaptoethanol	Sigma-Aldrich	M6250
GoTaq Green Master Mix	Promega	M7123
1 kb Plus DNA Ladder	NEB	N3200L
DNA Molecular Weight Marker VII, DIG-labeled	Sigma-Aldrich	11669940910
Precision Plus Protein™ All Blue Prestained Protein Standards	Bio-Rad	1610373
RNase A	Thermo Fisher Scientific	EN0531

(*Continued on next page*)

Continued

REAGENT or RESOURCE	SOURCE	IDENTIFIER
*Not*I-HF	NEB	R1389L
*Bbs*I-HF	NEB	R3539L
*Afe*I	NEB	R0652L
*Xho*I	NEB	R0146L
Amino-terminal FLAG-BAP™ Fusion Protein	Sigma-Aldrich	P7582
Dynabeads™ M-270 Epoxy	Invitrogen	14302D
Dynabeads™ Oligo($dT)_{25}$	Invitrogen	61005
SuperScript™ IV Reverse Transcriptase	Invitrogen	18090010
Agencourt RNAClean XP beads	Beckman Coulter	A63987
Critical commercial assays		
PureLink™ HiPure Plasmid Midiprep Kit	Invitrogen	K2100-15
Zyppy Plasmid Miniprep Kit	Zymo Research	D4037
Fungi/Yeast Genomic DNA Isolation Kit	Norgen	27300
Qubit dsDNA HS Assay Kit	Thermo Fisher Scientific	Q32854
Qubit dsDNA BR Assay Kit	Thermo Fisher Scientific	Q32850
NEBNext Ultra II FS DNA Library Kit	NEB	E7805
Zymo-Spin I Columns	Zymo Research	C1003
PALL 60207 Biodyne B High Sensitivity and Low Background Nylon Transfer Membrane, 0.45 μm Pore Size, 30 cm W x 3 m L Roll	Pall Corporation	60207
RNeasy Mini Kit	QIAGEN	74106
Qubit RNA BR Assay Kit	Thermo Fisher Scientific	Q10210
QIAseq Stranded Total RNA Library Kit	QIAGEN	180745
QIAseq FastSelect -rRNA Yeast Kit	QIAGEN	334217
NextSeq 500/550 High Output Kit v2.5 (75 Cycles)	Illumina	20024906
NextSeq 500/550 High Output Kit v2.5 (150 Cycles)	Illumina	20024907
MasterPure Yeast RNA Purification Kit	Lucigen	MPY03100
Agilent RNA 6000 Nano Kit	Agilent	5067–1511
Qubit RNA HS Assay Kit	Thermo Fisher Scientific	Q32852
Direct RNA Sequencing Kit	Oxford Nanopore Technologies	SQK-RNA002
Flow Cell Priming Kit	Oxford Nanopore Technologies	EXP-FLP001
MinION Flow Cell (R9.4.1)	Oxford Nanopore Technologies	FLO-MIN106D
Deposited data		
SynIX DNA and RNA sequences	This study	Sc2.0 umbrella: BioProject PRJNA351844 (https://www.ncbi.nlm.nih.gov/bioproject/PRJNA351844); *synIX*: BioProject PRJNA900304 (https://www.ncbi.nlm.nih.gov/bioproject/PRJNA900304)
Experimental models: Organisms/strains		
Saccharomyces cerevisiae: BY4741	Boeke laboratory	BY4741
All other strains used in this study are listed in Table S1	Boeke laboratory	Various, detailed in Table S1
Oligonucleotides		
PCRTag primers are listed in Table S2	Boeke laboratory	Various, detailed in Table S2

(*Continued on next page*)

Continued

REAGENT or RESOURCE	SOURCE	IDENTIFIER
Recombinant DNA		
See Tables S3–S7 for plasmids used in this study	Boeke laboratory	Various, detailed in Tables S3–S7
Software and algorithms		
GeneDesign	Boeke and Bader laboratories	Richardson et al.[40]
R	R Core Team	https://www.R-project.org/
Rstudio v1.3.1093	Rstudio	https://www.rstudio.com
Integrated Genomics Viewer (IGV) v2.7.2	Broad Institute[41]	http://software.broadinstitute.org/software/igv/
Image Studio Lite	LI-COR Biosciences	https://www.licor.com/bio/image-studio/
GraphPad Prism v9.4.0 for macOS	GraphPad Software	http://www.graphpad.com
Trimmomatic v0.39	Bolger et al.[42]	http://www.usadellab.org/cms/index.php?page=trimmomatic
FastQC v0.11.4	Andrews[43]	http://www.bioinformatics.babraham.ac.uk/projects/fastqc/
Bowtie 2 v2.2.9	Langmead and Salzberg[44]	http://bowtie-bio.sourceforge.net/bowtie2/index.shtml
ggplot2 v3.3.5	Wickham[45]	https://ggplot2.tidyverse.org/
Seqtk v1.3	N/A	https://github.com/lh3/seqtk/
Kallisto v0.46.0	Bray et al.[46]	https://pachterlab.github.io/kallisto/
STAR v2.5.2a	Dobin et al.[47]	https://github.com/alexdobin/STAR/
SAMtools v1.9	Li et al.[48]	http://samtools.sourceforge.net/
BEDtools v2.26.0	Quinlan et al.[49]	https://github.com/arq5x/bedtools2/
sleuth v0.30.0	Pimentel et al.[50]	https://pachterlab.github.io/sleuth/
Other		
Resource website for Sc2.0	Bader laboratory	https://syntheticyeast.github.io/

RESOURCE AVAILABILITY

Lead contact

Further information should be directed to and will be fulfilled by the lead contact, Jef D. Boeke (jef.boeke@nyulangone.org).

Materials availability

All unique/stable reagents generated in this study are available from the lead contact with a completed Materials Transfer Agreement.

Data and code availability

- Data: All data are available under the overarching Sc2.0 umbrella BioProject (PRJNA351844). The data for *synIX* are provided under BioProject PRJNA900304. The specific data reported here were deposited to Gene Expression Omnibus accession number GSE244153 for the RNA-seq data and Genbank Accession number CP125382 for the *synIX* sequence.
- Code: This work did not generate any code.
- Any additional information required to reanalyze the data reported in this paper is available from the lead contact upon request.

EXPERIMENTAL MODEL AND SUBJECT PARTICIPANT DETAILS

Yeast strains used in this work are listed in Table S1.

METHOD DETAILS

SynIX design

Design sequences for *synIX* were developed using BioStudio, according to the same guidelines used for designing the other synthetic chromosomes for Sc2.0. Designer sequences yeast_chr09_3_54 and yeast_chr09_3_55 were used as references for subsequent steps in the project. Version yeast_chr09_3_56 was developed after completion of yeast_chr09_9_02, and was used as a reference for final strain verification.

Yeast media

Yeast strains were cultured in rich medium (YPD) or synthetic complete (SC) medium with appropriate components "dropped out" e.g., SC–Ura lacks uracil. Yeast transformations were performed using lithium acetate protocols.[51] YPG plates used for growth assays contained 3% glycerol in place of dextrose as a carbon source. For expanded spot assays, the following media types were used: pH 4 and pH 8: pH of 2X YEP + dextrose adjusted using HCl and NaOH, respectively, before adding agar; camptothecin (Sigma-Aldrich, C9911): 0.1 μg/mL, 0.5 μg/mL, or 1.0 μg/mL in YPD; sorbitol (Sigma-Aldrich, S1876): 0.5 M, 1.0 M, 1.5 M, or 2.0 M in YPD; 6-azauracil (Sigma-Aldrich, A1757): 100 μg/mL in SC medium; hydroxyurea (Sigma-Aldrich, H8627): 0.2 M in YPD; MMS: methyl methanesulfonate (Sigma-Aldrich, 129925), 0.05% in YPD; benomyl (Sigma-Aldrich, 381586): 15 μg/mL in YPD; cycloheximide (Sigma-Aldrich, 01810): 10 μg/mL in YPD liquid medium for 2 h followed by plating to YPD; H_2O_2 (Millipore, 88597): 1 mM in YPD liquid medium for 2 h followed by plating to YPD. For chromoduction experiments, SC–Lys–Arg or SC–Leu–Arg plates were used with cycloheximide (10 μg/mL) and canavanine (12 μg/mL) added. For chromosome destabilization, strains were grown in YEP with 2% galactose and 1% raffinose added. Sporulation medium was prepared using a 50X base consisting of 50 g potassium acetate and 0.25 g zinc acetate dihydrate in 100 mL H_2O. Final 1X sporulation media was prepared from 2 mL of 50X sporulation medium base plus 300 μL of 10% yeast extract, 200 μM uracil, 2 mM leucine 300 μM histidine, and H_2O to 100 mL.

Minichunk assembly

Minichunks were originally assembled according to the following process, similar to the one previously described for *synIII*[5]: First, approximately 70-mer oligonucleotides with 20-mer overlaps were designed using GeneDesign software[40] and assembled by members of the Build-A-Genome class at Johns Hopkins University using polymerase cycling assembly (PCA) to produce 750 bp building blocks. Building blocks were verified by sequencing. Overlapping building blocks with approximately 40 bp overlaps were then assembled into 2–4 kb minichunks by direct homologous recombination in yeast. Minichunks were recovered from yeast into *E. coli*, and the recovered minichunk plasmids were verified by sequencing.

Later minichunks were ordered directly from DNA synthesis vendors with flanking *Not*I or *Bbs*I sites, verified by sequencing, excised from the vectors in which they were built via restriction digestion or, for those containing internal *Not*I or *Bbs*I sites, amplified by PCR, and integrated directly into the *synIX* strain or used for megachunk assembly.

Megachunk assembly and verification

Unlike the subsequent chromosomes, *synIX* was initially designed in separate "left and right" halves, which were subsequently merged. During the design process, *synIXL* was originally divided into megachunks A-F and V-Z. Following the integration of megachunks A-F as described in the "Minichunk integration by SwAP-In" section, the minichunks comprising megachunks V-Z in the original *synIX* design were reapportioned into three new megachunks, designated G, H, and I. Each megachunk plasmid was designed with flanking *Not*I sites for eventual excision of the assembled megachunk, 13–16 minichunks, a terminal selectable marker (*LEU2* or *URA3*, for use with SwAP-In), and homology arms between the first and last minichunks and the plasmid backbone. Overlaps between segments ranged from approximately 100-800 bp. Minichunks were released from their backbone plasmids or amplified by PCR, and were co-transformed with linkers and megachunk backbone plasmid into wild-type yeast (BY4741). Following plasmid assembly in yeast by homologous recombination and two days of growth on appropriate selective medium (SC–Leu or SC–Ura) at 30°C, single colonies were isolated and assessed by PCR to detect the presence or absence of each desired assembly junction. Colonies containing all desired junctions were recovered from yeast by phenol extraction and isopropanol precipitation, and subsequently electroporated into EPI300 *E. coli* cells (Lucigen, EC300150). Megachunk plasmids were extracted from *E. coli* using the PureLink HiPure Plasmid Midiprep Kit (Invitrogen, K2100-15).

To verify the sequences of the recovered megachunk plasmids, DNA sequencing libraries were prepared using 300 ng of plasmid DNA as input for the NEBNext Ultra II FS DNA Library Kit (NEB, E7805). DNA libraries were sequenced via Illumina NextSeq 500 using 36 bp pair-end reads. Following sequencing, reads were first processed using Trimmomatic v0.39[42] and FastQC v0.11.4,[43] aligned to an appropriate reference sequence using bowtie2 v2.2.9,[44] and visualized using IGV v2.7.2.[41]

Minichunk integration by SwAP-In

Minichunks were released from their backbones by restriction enzyme digestion, and the minichunks corresponding to one megachunk in the *synIX* design sequence (approximately 11–16 minichunks) were cotransformed into the partially completed *synIX* strain. Integration began at the left telomere of *chrIX* and proceeded in a stepwise fashion toward the centromere. At each step, the rightmost minichunk integrated contained either a *URA3* or a *LEU2* auxotrophic marker. These markers were alternated at each step according to the principles of Switching Auxotrophies Progressively for Integration (SwAP-In),[2,6] and colonies containing the new marker and lacking the previous strain's marker were identified by replica plating. Strains were assessed by PCRTag analysis after each round of integration.

Megachunk integration by SwAP-In

Sequence-verified megachunks were released from their assembly backbones via *Not*I digestion. Approximately 1 μg of digest product was transformed into the semisynthetic *synIX* strain, and cells were grown for two days at 30°C on appropriate SC dropout plates to select for the desired integration product. As with minichunk integration by SwAP-In, alternating *LEU2* and *URA3* auxotrophic

markers were used each round, enabling selection of colonies containing the desired new integration marker and a lack of the previous round's integration marker, as determined by replica plating. Colonies were assessed by PCRTag analysis, and colonies containing the desired PCRTags of interest were used for subsequent megachunk integration rounds. After integration of all three megachunks introduced by this method, yeast strain sequences were verified by whole genome sequencing, as described in the "Whole genome sequencing" section. To remove the *URA3* marker introduced during megachunk I integration, a PCR product with homology arms flanking *URA3* was transformed into the *synIX* strain, and colonies lacking the *URA3* marker were obtained following growth on 5-FOA medium.

PCRTag analysis

Cells from a single yeast colony were scraped from a plate using a pipette tip and resuspended in 30 μL of 20 mM NaOH in a 96-well PCR plate. The PCR plate was sealed and placed in a thermal cycler using the following boiling cycle: 3 cycles of 98°C for 3 min and 4°C for 1 min 1 μL of boiled product and 0.5 μM each primer were used in a 5 μL reaction using the GoTaq Green PCR system (Promega, M7123). An acoustic liquid handler (Labcyte, Echo 550) transferred primers and DNA template. Samples were run through the following protocol in a 384-well thermal cycler: 95°C for 5 min, 30 cycles of 95°C for 30 s, 55°C for 90 s, and 72°C for 60 s, and a final extension step of 72°C for 7 min. Samples were visualized following electrophoresis on a 1% agarose in 1X Tris-Taurine-EDTA gel containing ethidium bromide using the ChemiDoc XRS+ System (Bio-Rad).

Growth assays

A single yeast colony for each strain was inoculated into 5 mL YPD and incubated at 30°C overnight with rotation. For assays monitoring strain growth across multiple passages, overnight cultures were diluted 1:1000 in YPD and incubated at 30°C overnight with rotation until reaching the desired passage number. Overnight yeast culture was diluted to A_{600} = 0.15 into 6 mL of fresh YPD liquid medium and grown at 30°C with rotation until A_{600} reached 0.5–0.6. Cultures were serially diluted in 10-fold increments in H_2O, with a target OD of approximately 0.1 in 100 μL total volume for the first row of the wild-type control strain used to determine the starting culture volume in H_2O for each sample. 5 μL (YPD and YPG plates) or 10 μL (SC plates) of each dilution was spotted to each plate. Plates were grown at appropriate temperatures (room temperature of approximately 22°C on YPD, 30°C on YPD, YPG, and SC, and 37°C on YPD and YPG) and photographed daily. For additional media types (Figures S18 and S19), plates were prepared as described in the "Yeast media" section. Strains were serially diluted in 10-fold increments of H_2O as described above, and 5 μL of each dilution was spotted to each plate. Plates were grown at 30°C and photographed daily.

Plate reader growth assays in liquid culture

Three single yeast colonies per strain of interest were resuspended in 1 mL YPD in a 2 mL deep well plate and incubated for 24 h at 30°C with shaking at 800 rpm. Saturated cultures were diluted 1:100 in 200 μL YPD in a glass bottom 96-well plate with lid (Greiner Bio-One, 655892) and loaded into a Cytation 5 cell imaging multimode reader (Agilent). The following program was run using the Cytation 5 Gen5 software: 32 h at 37°C with continuous shaking, with A_{600} measured every 10 min. Data analysis and visualization were conducted using Microsoft Excel and GraphPad Prism 9.

Genome editing using CRISPR-Cas9

A two-plasmid system with one guide RNA (gRNA) plasmid and one Cas9 plasmid was used for most editing.[52] The Cas9 coding sequence was assembled together with a *TEF1* promoter and *CYC1* terminator in a pRS415 plasmid backbone (with *LEU2* marker). This plasmid was pre-transformed into yeast strains prior to the introduction of the gRNA plasmid and donor DNA. Guide RNA target sequences were selected by identifying 20 bp upstream of the desired protospacer adjacent motif (PAM) sequence (NGG). gRNAs were cloned into a 2-micron plasmid (pRS426, with *URA3* marker) under the control of a *SNR52* promoter using Gibson assembly. A modified version of the gRNA plasmid was used for editing two loci simultaneously. In this case, a second gRNA was cloned into the plasmid under control of a *RPR1* promoter and *RPR1* terminator. gRNA sequences were confirmed by Sanger sequencing (Genewiz). To edit the *synIX* strain, approximately 50 ng of gRNA plasmid and 200–300 fmol (for minichunk patch replacement) or 1 pmol (for point mutation fixing) of donor DNA were transformed into yeast cells containing the Cas9 plasmid. Cells were grown on dropout medium to select for the presence of both the Cas9 and gRNA plasmids, and editing was confirmed using either PCRTag analysis or PCR followed by Sanger sequencing (Genewiz).

Sporulation and tetrad dissection experiments for bug mapping

The *synIX* strain yLHM1192 was crossed to a wild-type yeast strain (BY4742 with a *URA3-pGAL-CEN9* cassette integrated near the centromere, also known as yLHM0539) to generate a heterozygous diploid (yLHM1233) with one copy of wild-type *chrIX* and one copy of *synIX*. To prepare strains for sporulation, a single colony of each strain was inoculated into 5 mL YPD and incubated at 30°C overnight with rotation. Overnight cultures were diluted to an OD of ~1 in YPD and grown to an OD of ~4, washed five times with H_2O, and resuspended in 2 mL of 1X sporulation medium. Strains were incubated at room temperature for 7–10 days with rotation, and monitored for the presence of tetrads. For tetrad dissection, 100 μL of these resuspended yeast cells in sporulation medium were washed and incubated with 25 μL of 0.5 mg/mL zymolyase in 1M sorbitol for 8 min 200 μL of 1M sorbitol was added to the cells, and 10 μL of the resulting mixture was added to a YPD plate. Tetrads were separated and picked using a dissection microscope

(Singer Instruments). Spores were grown for 2–3 days on YPD until visible colonies emerged. These strains were used for growth assays as described in the "Growth assays" section to classify each spore as healthy (similar fitness to the wild-type parent) or sick (similar fitness to the *synIX* parent). Strains from eighteen four-spore tetrads (72 strains) were prepared for whole genome sequencing, as described in the "Whole genome sequencing" section below.

Plasmid cloning and transformation for *synIX* bug mapping

Wild-type genes of interest plus approximately 500 bp of upstream flanking sequence and 200 bp of downstream flanking sequence were amplified from BY4741 by PCR. Genes were cloned into plasmid pRS413 linearized with *Afe*I by Gibson assembly and transformed into TOP10 cells. Colonies were grown up in 2 mL LB + 75 μg/mL carbenicillin and miniprepped using the Zyppy Plasmid Miniprep Kit (Zymo Research, D4037). Plasmid insert sequences were verified by Sanger sequencing. Plasmids were subsequently transformed into the *synIX* strain and grown for two days on SC–His plates. Yeast colonies containing each plasmid of interest were isolated, grown in SC–His liquid medium, and used for growth assays (as described in the "Growth assays" section) to assess their relative fitness compared to the starting *synIX* strain.

Selective destabilization and loss of one copy of *synIX* from disomic strain

A cassette containing a galactose-inducible centromere and a *URA3* marker (*URA3-pGAL-CEN9*) with homology arms matching *synIX* was amplified by PCR and transformed into the *synIX* strain. After two days of growth at 30°C on SC–Ura plates, single colonies were purified and assessed by junction PCR for the insertion of the *URA3-pGAL-CEN9* fragment. Strains were then grown in YEP +2% galactose +1% raffinose for two days and diluted to 5-FOA plates to obtain single colonies lacking *URA3*. Strains were single-colony purified and prepared for whole genome sequencing to assess chromosome copy number.

Whole genome sequencing

A single yeast colony was inoculated into 5 mL of YPD liquid medium at 30°C overnight with rotation. Overnight cultured yeast cells were harvested by centrifugation at 3000 x g for 3 min, and yeast genomic DNA was extracted using the Fungi/Yeast Genomic DNA Isolation Kit (Norgen, 27300). Genomic DNA concentration was determined using the Qubit dsDNA HS Assay Kit (Thermo Fisher Scientific, Q32854). DNA sequencing libraries were prepared using 300 ng of yeast genomic DNA as input for the NEBNext Ultra II FS DNA Library Kit (NEB, E7805). DNA libraries were sequenced via Illumina NextSeq 500 using either 75 bp or 36 bp pair-end reads. Following sequencing, reads were first processed using Trimmomatic v0.39[42] and FastQC v0.11.4,[43] aligned to an appropriate reference genome using bowtie2 v2.2.9,[44] and visualized using IGV v2.7.2.[41] Chromosome coverage plots were prepared in Rstudio version 1.3.1093 using the ggplot2 v3.3.5 package.[45]

Southern blot analysis

A single yeast colony was inoculated into 10 mL of YPD medium at 30°C overnight with rotation. Overnight cultured yeast cells were harvested by centrifugation at 3000 x g for 3 min, and yeast genomic DNA was extracted using the MasterPure Yeast DNA Purification Kit (Lucigen, MPY80200) according to the manufacturer's instructions, with an RNase A treatment step. DNA was quantified using the Qubit dsDNA BR Assay Kit (Thermo Fisher Scientific, Q32850). 2 μg of DNA were digested with *Xho*I at 37°C overnight. Digests were electrophoresed on a 1% Tris-Borate-EDTA gel in 0.5X Tris-Borate-EDTA running buffer for 10 h at 50V. Following electrophoresis, the gel was washed in depurination solution (0.25 M HCl) for 15 min, denaturation solution (0.5 M NaOH, 1.5 M NaCl) for 60 min, and neutralization solution (0.5 M Tris, 1.5 M NaCl, pH 7.5) for 30 min. Chromosomes were transferred by capillarity to a nylon membrane (Pall Corporation, 60207) using 10X SSC buffer (20X SSC: 1.5 M NaCl, 0.3 M sodium citrate, pH 7) for 18 h. After transfer, the membrane was washed in 2X SSC buffer for 5 min and baked at 80°C for 30 min. Prehybridization was performed for 60 min in ULTRAhyb Ultrasensitive Hybridization Buffer (Invitrogen, AM8669) at 55°C with rotation. For hybridization, probes were prepared by labeling a ~360 bp PCR fragment of universal telomere cap sequence from plasmid pJS160 using the PCR DIG Probe Synthesis Kit (Roche, 11636090910) with oligos 5′- GCTATACGAAGTTATTAGGGTAGTGTG-3′ and 5′- CTGCAGGTCGACTCTAGAGGATC-3′, according to the manufacturer's instructions. The following thermocycler conditions were used: 1 cycle of 95°C for 2 min, 30 cycles of 95°C for 30 s, 60°C for 30 s, and 72°C for 40 s, and a final elongation step of 72°C for 7 min. Probes were purified using Zymo-Spin I Columns (Zymo Research, C1003) and denatured at 95°C for 5 min. Hybridization was performed at 55°C overnight with rotation in 10 mL ULTRAhyb Ultrasensitive Hybridization Buffer (Invitrogen, AM8669) using 500 ng of probe per experiment. The blot was washed twice with 2X SSPE buffer (20X SSPE buffer: 0.02 M EDTA and 2.98 M NaCl in 0.2 M phosphate buffer, pH 7.4; Sigma-Aldrich, S2015) for 5 min at room temperature, twice with 2X SSPE +1% SDS for 30 min at 55°C, and twice with 0.1X SSPE for 15 min at 55°C. Blot was incubated overnight in 1:1 Intercept (TBS) Blocking Buffer (LI-COR Biosciences, 927–60001): 1X Tris-Buffered Saline (TBS) with 0.1% TWEEN 20 (Sigma-Aldrich, P1379) (1X TBST) and 1% SDS at room temperature. The next day, the membrane was washed with 1X TBST for 5 min and incubated for 1 h at room temperature with rabbit anti-DIG antibody (working concentration 1:2500 in 1:1 Intercept (TBS) Blocking Buffer: 1X TBST; Invitrogen, 700772). The primary antibody solution was washed out three times with 1X TBST for 15 min at room temperature. The membrane was incubated in goat anti-rabbit IgG secondary solution (LI-COR Biosciences, 926–68071, used at 1:10,000 in 1:1 Intercept (TBS) Blocking Buffer (LI-COR Biosciences, 927–60001): 1X TBST with 1% SDS) for 1.5 h. The blot was washed three times with 1X TBST for 15 min at room temperature plus one time with 1X TBS for 30 min at room temperature. An LI-COR Odyssey Instrument was used to develop the blot images.[53]

RNA extraction, sequencing, and analysis for short read sequencing

A single yeast colony was inoculated into 5 mL of YPD liquid medium at 30°C overnight with rotation. Overnight yeast culture was diluted to A_{600} = 0.15–0.2 into 6 mL of fresh YPD liquid medium and grown at 30°C or 37°C with rotation until A_{600} reached 0.8–1.0. Yeast cells were harvested from 4 mL of culture, and total RNA was extracted using the RNeasy Mini Kit (QIAGEN, 74106) according to the manufacturer's instructions. RNA was quantified using the Qubit BR RNA Assay Kit (Thermo Fisher Scientific, Q10210). 1 μg total RNA was used as input for the QIAseq Stranded Total RNA Library Kit (QIAGEN, 180745) plus QIAseq FastSelect -rRNA Yeast Kit (QIAGEN, 334217). RNA libraries were sequenced via Illumina NextSeq 500 using 75 bp paired-end reads. For applications requiring similar numbers of reads per sample, downsampling was performed using seqtk v1.3. Samples were first processed using Trimmomatic v0.39[42] and FastQC v0.11.4.[43] Processed reads were aligned to the S288C transcriptome and a custom *synIX* transcriptome (in which *chrIX* transcripts were replaced with their synthetic versions) using Kallisto v0.46.0[46] and STAR v2.5.2a.[47] STAR-aligned results were further processed using SAMtools v1.9[48] and BEDtools v2.26.0,[49] and visualized in IGV v2.7.2.[41] Kallisto pseudoalignment data was further processed in Rstudio version 1.3.1093 using the sleuth v0.30.0[50] and ggplot2 v3.3.5[45] packages. For volcano plots, we calculated effect scores (approximately log2 fold change values), tested results for significance using Wald's test, and corrected for multiple testing with the false discovery rate adjusted p value using the Benjamini-Hochberg method. The following genes deleted from the *synIX* design were removed from the plots in Figures 6D and 6E: *YIL173W* (*VTH1*), *YIL171W* (part of *HTX12* pseudogene), *YIL170W* (part of *HTX12* pseudogene), *YIL169C* (*CSS1*), *YIL167W* (*SDL1*, blocked reading frame), *YIL082W*, *YIL060W*, *YIL059C*, *YIL058W*, *YILWTy3-1*, *YILCdelta3*. The following dubious ORFs, retrotransposable elements, and subtelomeric genes were also removed: *YBL100C*, *YGR296C-B*, *YHL050W-A*, *YHR219C-A*, *YIL020C-A*, *YJR029W*, *YLL066C*, *YML133W-B*, *YMR046C*, *YNL339W-B*, *YNL339C*, *YOR277C*, *YPL283W-B*, *YPR158W-B*, *YPR204C-A*, *YBLWdelta4*, *YCLWdelta3*. Unfiltered versions of the volcano plots are depicted in Figure S20.

RNA extraction, sequencing, and analysis for nanopore direct RNA sequencing

Methods recently described by us were used to perform nanopore sequencing to analyze RNA isoforms.[54] Total RNA was extracted from 50 mL flash-frozen cell pellets grown to mid-log (OD_{600} ~0.65–0.85) using the MasterPure Yeast RNA Purification Kit (Lucigen) including a DNase I treatment step. RNA (diluted 1:10) quality and concentration were measured by Agilent 2100 Bioanalyzer with the Agilent RNA 6000 Nano Kit and Qubit RNA High Sensitivity Kit (Thermo Fisher Scientific), respectively. Poly(A) mRNA was enriched from 50 μg total RNA on 132 μL Dynabeads oligo$(dT)_{25}$ beads. The Direct RNA Sequencing Kit (SQK-RNA002, Oxford Nanopore Technologies) was used to generate libraries from 500 ng poly(A) RNA. An optional reverse transcription was performed at 50°C for 50 min using SuperScript IV Reverse Transcriptase (Invitrogen) in between the ligation of the RTA and RMX adaptors. Following reverse transcription the RNA:cDNA was cleaned up with 1.8 volumes of Agencourt RNAClean XP beads and washed with 70% ethanol. Following RMX ligation only one volume of beads was used in the clean-up, and WSB (SQK-RNA002) was used in the wash steps. Direct RNA libraries (typically 150–200 ng) were loaded onto primed (EXP-FLP001) MinION flow cells (FLO-MIN106D, R9 version) in RRB buffer and run on the GridION with MinKNOW 5.2.2 for up to 72 h. Nanopore long reads were base-called, trimmed of adapter sequences, and filtered for quality, retaining only those with the best alignment scores for multi-mapping reads, as previously described.[54] For TSS distributions, long-reads that overlapped at least 75% of the annotated gene were used.

Construction of FLAG-tagged *EST3* strains

A DNA fragment containing a six-glycine linker plus a 3X FLAG tag (DYKDHDG-DYKDHDI-DYKDDDDK) was designed for integration at the 3′ end of *EST3*, in-frame with the rest of the protein and inserted just before the *EST3* stop codon. The segment containing the tag was flanked by 70–100 bp homology arms matching the yeast genome sequence adjacent to the desired insertion site. Genome editing using CRISPR-Cas9 in yeast (as describe above) was used to cut the genome near the end of the *EST3* coding sequence and insert the tag of interest. Colony PCR and Sanger sequencing (Genewiz) were used to confirm in-frame insertion of the tag.

Immunoblot analysis

A single yeast colony was inoculated into 5 mL of YPD liquid medium at 37°C overnight with rotation. Overnight culture was diluted to A_{600} = 0.15–0.2 into 50 mL of fresh YPD liquid medium and grown at 37°C with shaking at 200 rpm until A_{600} reached 0.8–1.0. Yeast were harvested by centrifugation, and pellets were frozen overnight at −80°C. Pellets were subsequently resuspended in 500 μL of lysis buffer (20 mM HEPES pH 7.4, 1% Triton X-100 (Sigma-Aldrich, X100), 2 mM $MgCl_2$, 500 μM NaCl, and 1X protease inhibitor (Roche)). Cell suspension was added to MP Biomedicals FastPrep Lysing Matrix C and subjected to the following shaking program at 4°C using a FastPrep-24 5G (MP Biomedicals): 7 cycles of 15 s shaking at 6.0 m/s + 30 s rest between cycles. Samples were centrifuged at 13000 x g for 10 min at 4°C, and 30 μL of supernatant was transferred to a new tube and mixed with 10 μL of 4X LDS loading buffer (Invitrogen, NP0007) (pre-immunoprecipitation sample). The remaining supernatant was transferred to pre-equilibrated FLAG M2 (Sigma F1804)-conjugated M-270 Dynabeads (Invitrogen, 14302D) for immunoprecipitation.[55] Samples with beads were incubated on ice for 60 min, washed 3 times with lysis buffer, and eluted at 70°C with shaking at 700 rpm in 50 μL 1.1X LDS loading buffer (Invitrogen, NP0007) in lysis buffer for 10 min 2-mercaptoethanol (1.43 M final) was added, and samples were heated to 95°C for 5 min and loaded onto an SDS-PAGE gel for immunoblotting. Mouse anti-FLAG M2 antibody (Sigma F1804, used at 1:5000) and rabbit anti-histone H3 antibody (Abcam, 1791, used at 1:5000) were used for blotting proteins of interest overnight at 4°C. Goat anti-mouse IgG1 (LI-COR Biosciences, 926–32350, used at 1:20,000) and goat anti-rabbit IgG (LI-COR Biosciences, 926–68071, used at 1:20,000)

were used for blotting FLAG and H3 primary antibodies, respectively, during a 1-h incubation at room temperature. An LI-COR Odyssey Instrument was used to develop the blot images.[53]

Pulsed-field gel electrophoresis

A single yeast colony was inoculated into 7 mL of YPD liquid medium and grown at 30°C for two days with rotation. Approximately 40 mg of yeast cells were harvested by centrifugation. To prepare plugs, 16 μL of zymolyase solution (25 mg/mL zymolyase 20T in 10 mM KH_2PO_2 pH 7.5) and 360 μL of 0.5% melted low melting point agarose (Bio-Rad, 1620137) in 100 mM EDTA pH 7.5 were added to the cell pellet and mixed by pipetting. 90 μL of this suspension was added per well of a BioRad plug mold, and the plugs were cooled for 30 min at 4°C. Solidified plugs were then transferred into 15 mL tubes containing 1 mL of digestion buffer (0.5 M EDTA, 10 mM Tris, pH 7.5), mixed by inversion, and incubated at 37°C with rotation overnight. The next day, 400 μL of proteinase K solution (5% sarcosyl and 5 mg/mL proteinase K in 0.5 M EDTA, pH 7.5) were added to the tube. Samples were incubated at 50°C for 5 h, and then washed once with H_2O and three times with TE (2 mM Tris, 1 mM EDTA, pH 8.0). Plugs were stored at 4°C until ready for gel loading. Half of one plug per sample was embedded per well of a gel consisting of 1% low melting point agarose in 0.5X Tris-Borate-EDTA buffer. Samples were separated in running buffer of 0.5X Tris-Borate-EDTA by clamped homogeneous electric field gel electrophoresis using the CHEF Mapper XA Pulsed-Field Electrophoresis System (Bio-Rad), as previously described.[56] The following program was used: auto-algorithm with size range of 200 kb to 2.5 Mb, temperature of 14°C, voltage of 6 V/cm, included angle of 120°. After electrophoresis, gels were stained using 5 μg/mL ethidium bromide in H_2O for 30 min, destained in H_2O for 30 min, and then imaged using the ChemiDoc XRS+ System (Bio-Rad).

Chromosome substitution and conditional centromere destabilization

For initial experiments, disomic *synIX* strain yLHM0387 was used as the donor and yWZ601 as the recipient for *kar1-1*-mediated chromoduction. For follow-up experiments, disomic strain yLHM0604 and monosomic strains yLHM0721, yLHM1591, and yLHM1601 were used as donors and yWZ602 as the recipient for *kar1-1*-mediated chromoduction. yWZ601 and yWZ602 were derived from DMy044[25] following deletion of *LYS12* from wild-type *chrIX* and insertion of a *URA3-pGAL* promoter cassette upstream of *CEN9*.[27] Strains were grown independently on YPD plates, and subsequently mated on YPD plates via replica plating. After 14 h of growth, these plates were replica plated to SC–Lys–Arg plates with 12 μg/mL canavanine and 10 μg/mL cycloheximide added. Plates were grown until individual colonies emerged; if a patched formed instead, patches were replica plated to the same selective medium and grown for additional time until individual colonies emerged. Single colonies were restreaked to fresh selective plates and analyzed by PCRTagging, pulsed-field gel electrophoresis, and whole genome sequencing. To lose wild-type *chrIX*, strains were grown in YPD overnight, diluted 1:1000 in YEP +2% galactose medium for 24 h, and plated on 5-FOA medium to select for strains that had lost wild-type *chrIX*. Single colonies were genotyped by PCRTag analysis and further characterized by pulsed-field gel electrophoresis and whole genome sequencing. For chromosome substitution to move *synIX* from yLHM1601 to recipient strain yLHM2231 (derived from BY4742), a *LEU2* marker was integrated into *synIX* near the end of megachunk H, in minichunk 101, generating strain yLHM1754. The same protocol as listed above was followed using donor strain yLHM1754 and recipient strain yLHM2231, except after mating and 14 h of growth, plates were replica plated to SC–Leu–Arg (rather than SC–Lys–Arg) plates with 12 μg/mL canavanine and 10 μg/mL cycloheximide added.

QUANTIFICATION AND STATISTICAL ANALYSIS

Information on the number of biological replicates, statistical tests, and p values used is provided in the Figure legends and "Method Details" section.